Cell Metabolism

Article

Methionine-supplemented longevity diet increases growth hormone, GLP-1, and FGF21; reduces frailty; and promotes healthspan

Graphical abstract

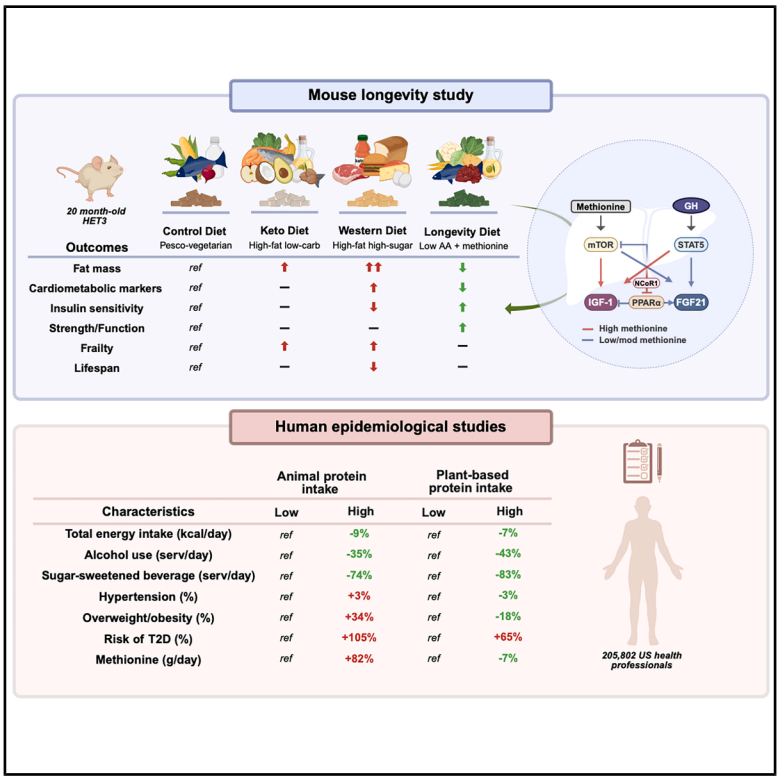

Highlights

- Western and keto diets increase fat mass and frailty and reduce healthspan in aged mice
- A low-amino-acid, moderate-methionine longevity diet promotes health and reduces frailty
- Higher animal protein/EAA intake is associated with increased obesity and T2D risk

Authors

Maura Fanti, Sebastian Brandhorst, Gerardo Navarrete, ..., Vasanti S. Malik, Frank B. Hu, Valter D. Longo

Correspondence

vlongo@usc.edu

In brief

Fanti et al. show that a low-protein, pescatarian longevity diet, inspired by traditional dietary habits in areas of exceptional longevity and supplemented with moderate methionine, increases GH, FGF21, and GLP-1; enhances cardiometabolic health and insulin sensitivity; and reduces fat mass without causing lean mass loss or requiring calorie restriction.

Fanti et al., 2026, Cell Metabolism *38*, 1–20
August 4, 2026
https://doi.org/10.1016/j.cmet.2026.05.015

CellPress

Cell Metabolism

CellPress

Article

Methionine-supplemented longevity diet increases growth hormone, GLP-1, and FGF21; reduces frailty; and promotes healthspan

Maura Fanti,[1] Sebastian Brandhorst,[1] Gerardo Navarrete,[1] Arnold Diaz,[1] Giacomo Giuliani,[1] Dolly Chowdhury,[1] Gabriel C. Antunes,[2] Todd E. Morgan,[1] Louis Dubeau,[3] Valentina Villani,[4] Laura Perin,[4,5] Vasanti S. Malik,[6,7] Frank B. Hu,[7,8] and Valter D. Longo[1,9,*]

[1]Longevity Institute, Leonard Davis School of Gerontology, University of Southern California, Los Angeles, CA, USA
[2]Laboratory of Molecular Biology of Exercise, University of Campinas, Limeira, São Paulo, Brazil
[3]Department of Pathology, Keck School of Medicine, University of Southern California, Los Angeles, CA, USA
[4]GOFARR Laboratory, Children's Hospital Los Angeles, Division of Urology, Saban Research Institute, Los Angeles, CA, USA
[5]Department of Surgery, Keck School of Medicine, University of Southern California, Los Angeles, CA, USA
[6]Department of Nutritional Sciences, University of Toronto, Toronto, ON, Canada
[7]Department of Nutrition, Harvard T.H. Chan School of Public Health, Boston, MA, USA
[8]Department of Epidemiology, Harvard T.H. Chan School of Public Health, Boston, MA, USA
[9]Lead contact
*Correspondence: vlongo@usc.edu
https://doi.org/10.1016/j.cmet.2026.05.015

SUMMARY

Southern European countries have some of the highest life expectancies in the world, yet they display relatively high frailty. We examined different diets to identify compositions that promote both healthspan and strength in mice. The western and ketogenic diets increased fat mass and frailty and increased either cholesterol or insulin resistance, whereas a low-protein longevity diet, modeling the traditional Mediterranean and Okinawan diets but supplemented with methionine (LDMM), reduced fat mass and frailty while improving cardiometabolic markers. LDMM reduced insulin-like growth factor (IGF)-1 while increasing growth hormone, GLP-1, and fibroblast growth factor (FGF)21, which was required for fat loss and insulin sensitivity. Bimonthly cycles of a 4-day fasting-mimicking diet instead improved metabolic markers. A cross-sectional analysis of epidemiological data from over 200,000 men and women indicates that those with the highest animal protein intake tended to have a healthier lifestyle but had approximately double the prevalence of type 2 diabetes compared with those in the lowest intake group. These findings indicate that mostly plant-based low-amino-acid diets have the most potent effects on healthspan but require moderate methionine intake to minimize frailty.

INTRODUCTION

Pharmacological treatments, particularly GLP-1 agonists, have demonstrated remarkable effectiveness in managing type 2 diabetes (T2D) and promoting weight loss,[1] but side effects, including lean mass loss, gastrointestinal problems, and ischemic optic neuropathy,[2–5] contribute to a high percentage of patients discontinuing the treatment within 3 years with subsequent weight regain, limiting their potential as feasible treatments to extend lifespan and healthspan and reduce frailty.[6] Therefore, an ideal healthspan-extending intervention should (1) prevent or reverse overweight/obesity, (2) slow down aging , (3) minimize frailty and other side effects, and (4) allow long-term compliance.

Dietary patterns adopted by populations consistently ranked among those with the highest life expectancy,[7–9] such as the mostly plant-based traditional diets of Japan[10] or of Mediterranean areas,[11–13] do not require the severe calorie restriction known to extend longevity and healthspan in various organisms, including rodents[14] and monkeys,[15] and to lower disease risk factors in humans.[16,17] Nevertheless, the adoption of the traditional Mediterranean diet continues to decline[18,19] due to a dietary "westernization" trend and, in part, to its perceived association with lean mass loss.[20] In fact, Southern Europe has been reported to have a higher proportion of frail elderly individuals than most countries in Central and Northern Europe.[21]

To identify a dietary pattern that promotes longevity and healthspan while minimizing frailty, we evaluated the effects of *ad libitum* administration of various nutritional regimens started late in life (at 20 months of age) in female and male genetically heterozygous HET3 mice. We developed a new, low-amino-acid, high-carbohydrate, and relatively high-fat diet formulation,

Please cite this article in press as: Fanti et al., Methionine-supplemented longevity diet increases growth hormone, GLP-1, and FGF21; reduces frailty; and promotes healthspan, Cell Metabolism (2026), https://doi.org/10.1016/j.cmet.2026.05.015

which we termed the "longevity diet" (LD) based on previous animal studies, epidemiological studies, clinical studies, and traditional diets adopted by populations in different areas known for exceptional longevity—particularly those in Italy, Greece, Spain,[11,13] and Japan.[9] We compared its effects on healthspan with those of a healthy control diet, a typical western diet (WD) high in processed sugars and fats, and a healthy ketogenic diet (KD) high in unsaturated fats, low in protein, and very low in carbohydrates. We also assessed the effects of a periodic 4-day fasting-mimicking diet in HET3 mice.

RESULTS

Study design

We set up a cohort of 40–44 females and 40–44 males per group of genetically heterogeneous UM-HET3 mice for a lifespan study. An additional cohort of 30 female and 16–20 male mice underwent healthspan assessments (including metabolic, frailty, and cognitive evaluations) within 6 months of intervention (Figure 1A). Mice were enrolled in the study at 20 months of age, a stage of life comparable to that of a 60- to 65-year-old person. HET3 mice were chosen because they represent the ideal model for lifespan and healthspan studies.[22] The experimental groups received a control standard diet (SD), a WD, a KD, and an LD, followed within 2 weeks by a switch to the same LD supplemented with moderate levels of methionine (LDMM) or two 4-day cycles of a fasting-mimicking diet (FMD) per month combined with an SD for the rest of the month (Table S1). Based on a pilot experiment (Figure 1B), in which female HET3 mice fed the low-amino-acid LD experienced rapid weight loss, we supplemented the LD to achieve a moderate methionine level (LDMM) and to protect against further weight loss. In fact, methionine is a precursor to S-adenosylmethionine (SAM), which is essential in anabolic processes and decreases in skeletal muscle with aging.[23] Moreover, disrupted methionine metabolism can trigger muscle atrophy, while methionine supplementation can turn off muscle-wasting genes and reduce oxidative stress, helping to prevent lean mass loss.[24,25] Although the amino acid-restricted LD has the potential to extend lifespan, we did not continue the lifespan experiment with this diet due to institutional animal care regulations. Therefore, after a very short period on the LD (methionine 0.14%; cystine 0.14%), which varies from 1 to a few weeks based on body weight (BW) loss, mice were switched to the methionine-supplemented LDMM (methionine 0.3%; cystine 0.14%) (LD → LDMM), which stabilized BW (Figure 1B). An average weight loss of 20% was chosen as the criterion for transition between LD and LDMM formulations for ethical reasons and to minimize frailty. Of note, the effect of 1 month of LDMM in C57BL/6J mice on weight loss, fat mass, and fasting blood glucose was similar to that in HET3 mice, although it took longer to achieve (Figures S1A–S1C).

Methionine-restricted (MetR) diets are well established to extend lifespan and promote healthy aging, even when started late in life.[26–29] Notably, the LDMM is not a MetR diet, as it contains nearly twice the methionine content of those used in typical MetR studies,[29] plus 0.14% cystine, which is absent in typical MetR diets because it can be broken down into cysteine to function in the methionine-cysteine pathway.[30,31] LDMM instead contains about ½ of all amino acids but more than twice the fat of the control diet (Tables S1 and S2). LDMM, which models the traditional southern Italian/Mediterranean diet but also the diets of other Mediterranean countries, as well as Okinawa, is rich in vegetables, legumes, potatoes, and olive oil but also contains a limited amount of fish meal (Table S1), which explains its low-protein/amino acid content. The control diet, instead, is rich in ground corn, ground wheat, ground oats, soybean oil, dried beet pulp, soybean meal, fish meal, and dried whey (Table S1).

As the study did not show significant differences between sexes, we present data from the female cohort unless otherwise stated. Results for males only or combined males and females can be found in the supplemental information.

Effect of dietary interventions on cardiometabolic biomarkers and body composition

Initially, WDs and KDs caused weight gain (Figure 1C). In contrast, despite similar energy density compared with the SD group (Table S1), the LD group showed a rapid decrease in BW, which was stabilized by methionine supplementation for the remainder of the study (LDMM) (Figure 1C). Similar effects on weight loss and fasting blood glucose were observed with LDMM alone in a short-term experiment in C57BL/6 mice (Figures S1A–S1C). Mice subjected to twice-monthly FMD cycles maintained a relatively low weight after recovering from each cycle. Except for the FMD group, which followed a periodically restricted program, the other groups maintained a constant food/energy intake (Figure S1D). Mice initially fed the LD and, 1–2 weeks later, switched to the LDMM displayed increased appetite, consistent with the literature on MetR dietary studies.[32] NMR analysis showed that body composition remodeling occurred almost exclusively at the expense of fat mass (Figures 1D, S1E, and S1F). Whereas SD mice had minor changes in BW and fat mass, WD and KD mice increased fat mass compared with the SD ($p = 0.008$ and $p = 0.02$), LDMM ($p < 0.0001$ for both), and FMD ($p < 0.0001$ for both) cohorts. LDMM mice showed the strongest fat mass reduction ($p < 0.0001$ for all comparisons) but no lean mass loss (Figure 1D). Considering the physiological decline in body composition that generally occurs with age,[33] lean mass was preserved in all groups at 23 months of age (Figure 1D). The LDMM group exhibited the lowest grams of fat per gram of lean mass (Figure S1G).

After 5 months, the dietary interventions markedly influenced cardiometabolic markers (Figures 1E–1I). Compared with the SD cohort, the LDMM and FMD cohorts reduced glucose levels ($p < 0.0001$ and $p = 0.02$) (Figure 1E). KD, LDMM, and FMD cohorts showed slight but non-significant increases in beta-hydroxybutyrate (BHB; Figure 1E). Insulin levels were increased only in the KD group. Insulin resistance (HOMA-IR) increased in the KD compared with the LDMM group ($p = 0.03$) (Figure 1F). In line with previous clinical findings,[34] an adiponectin increase was observed only in the FMD group (Figure 1G). Furthermore, leptin levels were low in the LDMM group and slightly reduced in the FMD cohort, but high in the WD group, likely reflecting leptin resistance. Total cholesterol and LDL, but not HDL, levels were increased in the WD and KD cohorts (Figure 1H), resulting in LDL/HDL ratios above 4, which are recognized as a risk factor for cardiovascular disease in humans

Please cite this article in press as: Fanti et al., Methionine-supplemented longevity diet increases growth hormone, GLP-1, and FGF21; reduces frailty; and promotes healthspan, Cell Metabolism (2026), https://doi.org/10.1016/j.cmet.2026.05.015

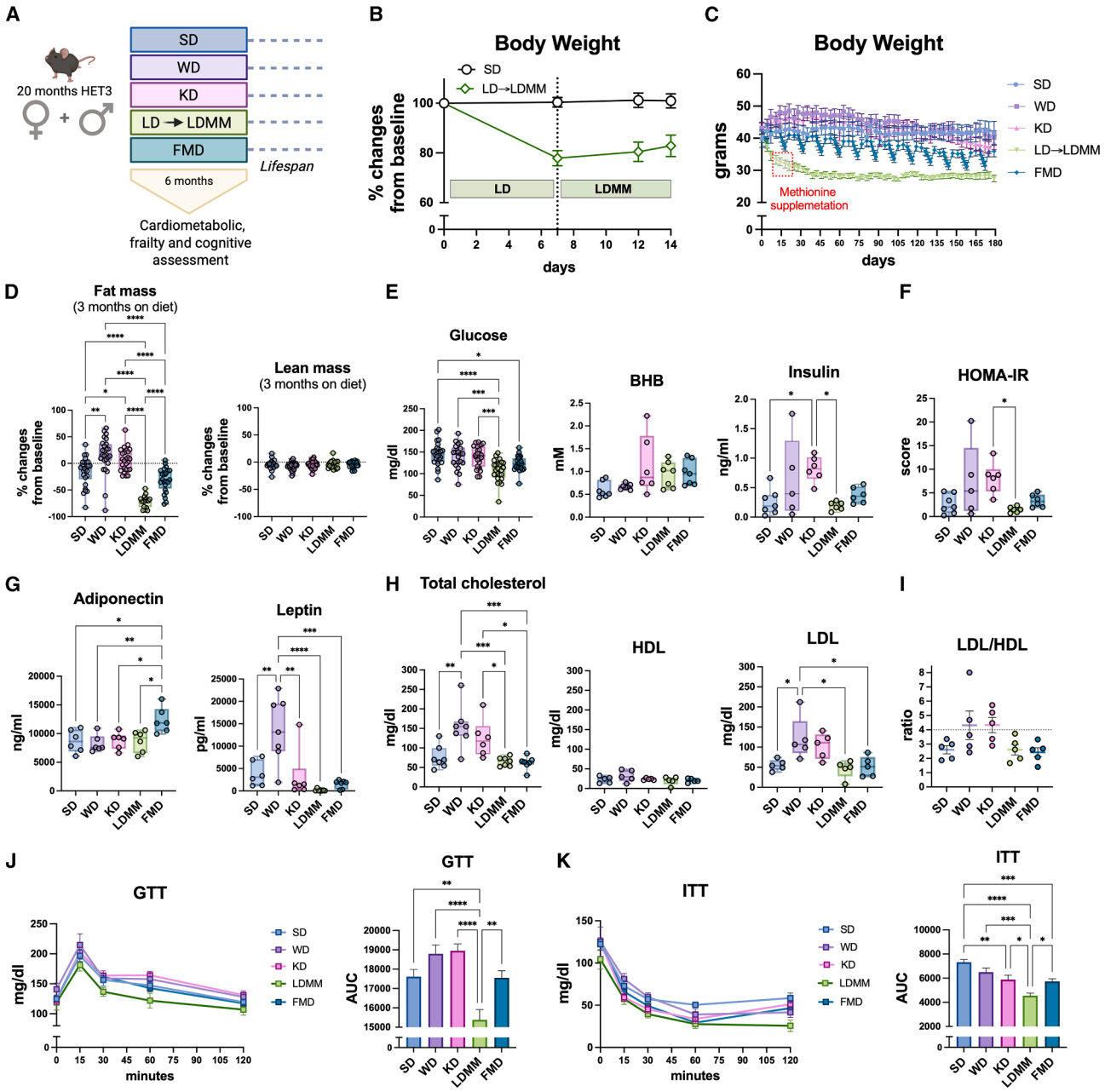

Figure 1. Dietary interventions affect cardiometabolic markers and body composition in HET3 mice

(A) Overview of the experimental design involving female and male HET3 mice in the lifespan study (n = 40–44/group) and assessment of metabolic, frailty, and cognitive decline (female n = 30/group; male n = 15–20/group). The mice entered the study at 20 months of age.

(B) LD methionine supplementation (LD → LDMM) stabilizes body weight (BW) in female HET3 mice (n = 5–6/group).

(C) BW (g) changes over 6 months of dietary intervention in female HET3 mice (n = 20–24/group).

(D) Changes in fat and lean mass (% change from baseline) after 3 months on diets in female HET3 mice (n = 17–26/group).

(E–I) Circulating markers for glucose and lipid metabolism, including insulin resistance (HOMA-IR) and risk factors for cardiovascular diseases (LDL/HDL), were measured after 5 months on the diets in female HET3 mice (glucose, n = 21–26/group; other markers, n = 5–7/group).

(J and K) (J) GTT (n = 10–13/group) and (K) ITT (n = 6–9/group) were performed after 4 months of diets in female HET3 mice.

(D–K) Mice in the LDMM group received LD for 1–2 weeks before switching to the LDMM.

Data are presented as mean ± SEM. $^{*}p < 0.05$, $^{**}p < 0.01$, $^{***}p < 0.001$, $^{****}p < 0.0001$ indicate statistical significance calculated by one-way ANOVA followed by Tukey multiple comparison test or using Kruskal-Wallis test followed by Dunn's multiple comparisons test. The illustration was created with BioRender.

See also Figure S1.

Please cite this article in press as: Fanti et al., Methionine-supplemented longevity diet increases growth hormone, GLP-1, and FGF21; reduces frailty; and promotes healthspan, Cell Metabolism (2026), https://doi.org/10.1016/j.cmet.2026.05.015

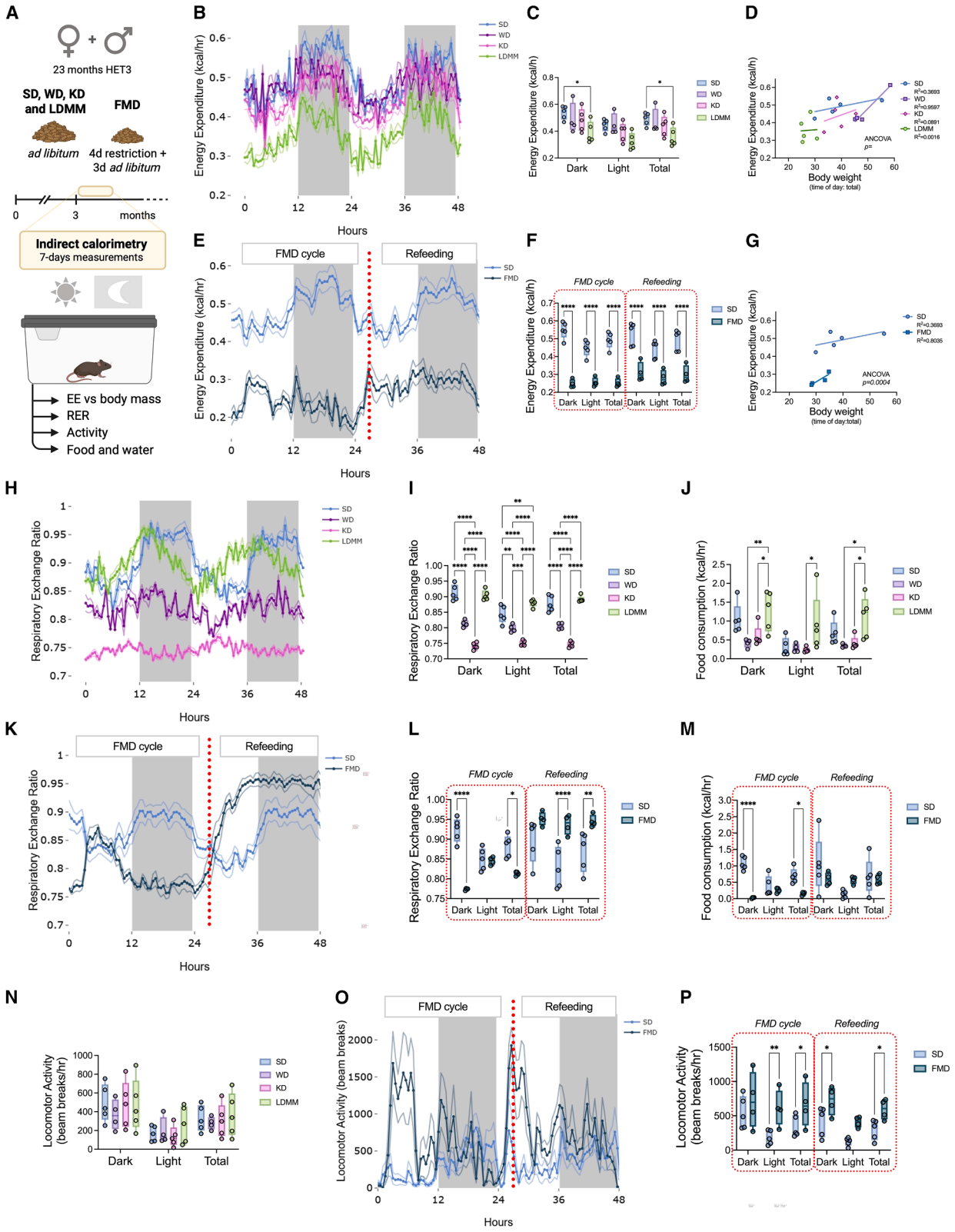

Figure 2. Metabolic assessment of female HET3 mice in response to dietary interventions

(A) Overview of metabolic assessment over 7-day measurements in female and male HET3 mice (n = 4–6/group). After 3 months of continuous diets (SD, WD, KD, and LDMM) or 6 cycles of FMD, the mice were placed in metabolic cages.

(legend continued on next page)

(Figure 1I). Glucose and insulin tolerance tests (GTT and ITT), performed on 24-month-old mice after 4 months on the diets (Figures 1J and 1K), indicated that glycemic control and insulin sensitivity significantly improved in LDMM-fed mice compared with all other groups, including mice on the SD (GTT, $p = 0.002$; ITT, $p < 0.0001$) (Figure 1I). Insulin sensitivity was also enhanced in the FMD compared with the SD group ($p = 0.0004$), aligning with the FMD's effect on the insulin sensitizer adiponectin (Figure 1G). Interestingly, the SD group exhibited reduced insulin tolerance compared with the KD group ($p = 0.004$) (Figure 1K).

In summary, 4–5 months of LDMM or FMD cycles improved cardiometabolic markers/risk factors compared with the SD, whereas both WD and KD increased these risk factors. In males, body composition (Figures S1E and S1F) and glucose metabolism markers exhibited a similar trend (Figures S1H and S1I). Interestingly, in KD-fed mice, glucose tolerance was significantly impaired compared with that in the SD ($p = 0.04$), WD ($p = 0.04$), and LDMM ($p < 0.0001$) groups (Figure S1H).

Metabolic assessment of HET3 mice in response to dietary interventions

We investigated the effects of the dietary interventions on food and water intake, energy expenditure (EE), respiratory exchange ratio (RER), and ambulatory activity counts at 23 months[35] (Figure 2A).

Heavier mice generally burn more calories than leaner mice to support the energy demands of higher basal metabolic rates and physical activity.[37] Although LDMM mice exhibited lower EE (kcal/h) (Figures 2B, 2C, and S2A), analysis of covariance (ANCOVA) adjusted for body mass found no significant differences in EE among SD, WD, KD, and LDMM mice (Figure 2D), indicating comparable EE relative to body mass across groups. Predictably, decreased EE during the FMD cycle ($p < 0.0001$), which increased during refeeding (Figures 2E–2G and S2B), aligns with a metabolic shift toward energy conservation during fasting. EE showed consistency across sexes (Figures S2C and S2D). Dietary manipulation significantly altered RER in both female and male HET3 mice (Figures 2H, 2I, S2E, and S2F). As expected, KD mice displayed persistently lower RER values compared with all other groups (total: $p < 0.0001$ for all comparisons) (Figure 2I), consistent with higher lipid oxidation. WD mice showed an intermediate RER, lower than that of SD and LDMM mice (total: $p < 0.0001$ for both comparisons) (Figure 2I). The SD and LDMM groups exhibited similar RER during the dark (active) phase, with LDMM mice showing a higher RER than SD mice during the light (inactive) phase (Figure 2I), indicating a mostly carbohydrate-dependent metabolism. This can be explained by the non-significant trend toward increased food intake during the inactive phase in LDMM mice compared with their SD counterparts ($p = 0.06$; Figure 2J), which remains higher than that in KD mice (light: $p = 0.03$). Sustained higher RER levels are not consistent with a fasted state, indicating compensatory feeding behavior and potentially connecting substrate utilization to appetite regulation. Mice in the LDMM group consumed more calories than those in the WD and KD groups (total: $p = 0.02$ and $p = 0.03$) (Figures 2J, S2G, and S2H).

These findings support the hypothesis that lower BW in the LDMM group occurs independently of calorie restriction. On the contrary, the FMD cycle resulted in a marked reduction in RER (total: $p = 0.02$) (Figures 2K, 2L, S2I, and S2J), consistent with food restriction and increased lipid oxidation (Figures 2M, S2K, and S2L). As expected, during refeeding, RER increased rapidly (total: $p = 0.008$) (Figure 2L), indicating a return to carbohydrate utilization (Figure 2M). The RER was consistent between females and males (Figures S2F–S2J). Mice in the WD, KD, and FMD groups (only during the FMD cycle) exhibited reduced water intake in the active phase compared with those in the SD group ($p = 0.004$, $p = 0.01$, and $p = 0.0008$) (Figures S2M–S2P). Finally, no differences in locomotor activity were found among the SD, LDMM, and KD groups, whereas a trend toward reduced activity was observed in the WD cohort, which sustained the weight gain (Figures 2N and S2Q). Locomotor activity was instead increased during the FMD cycle and refeeding

(B–P) Mice in the LDMM group received LD for 1–2 weeks before switching to the LDMM. Plots of energy expenditure (EE, kcal/h), respiratory exchange ratio (RER, VCO_2/VO_2), activity (total beam breaks, XT + YT), and statistical analysis over 167 h (gray bars indicate dark photoperiods). Due to limited space, the figure shows time plots of the data over 48 h. The complete 167-h measurement is available in the supplemental information.

(B–D) EE versus time in SD, WD, LD, and LDMM. The boxplot shows EE as the average over 7 light-dark cycles in SD, WD, LD, and LDMM. Points represent individual mice. ANCOVA for EE with body mass as covariate shows no significant difference between SD, WD, KD, and LDMM groups. A mass × diet interaction effect was not significant.

(E–G) EE versus time in FMD showing the transition from the last day of FMD to the first day of refeeding. The boxplot shows EE as the average over 4 light-dark cycles in FMD, and 3 light-dark cycles during refeeding. ANCOVA for EE, with body mass as covariate, showed a significant difference between the SD and FMD groups. A mass × diet interaction effect was not significant.

(H and I) RER versus time in SD, WD, LD, and LDMM. The boxplot shows RER as the average over 7 light-dark cycles.

(J) Food consumption (kcal/h) in SD, WD, LD, and LDMM. Due to the LDMM pellet's tendency to crumble, we used special feeders in the standard cages (STAR Methods) to prevent food spillage and confirmed a notably high calorie intake in the LDMM group.

(K and L) RER versus time in FMD showing the transition from the last day of FMD to the first day of refeeding. The boxplot shows RER as the average over 4 light-dark cycles in FMD, and 3 light-dark cycles during refeeding.

(M) Food consumption (kcal/h) as the average over 4 light-dark cycles in FMD, and 3 light-dark cycles during refeeding.

(N) Locomotor activity (total beam breaks) as the average over 7 light-dark cycles in SD, WD, LD, and LDMM.

(O) Locomotor activity (total beam breaks) versus time in FMD, showing the transition between the last day of FMD and the first day of refeeding.

(P) Locomotor activity (total beam breaks) as the average over 4 light-dark cycles of FMD and 3 light-dark cycles during.

Indirect calorimetry data were analyzed using the CalR app[36] to calculate EE and correct for body mass. Data versus time is plotted as the group means for each diet ± SEM, as represented by the line and ribbon, respectively. Data are plotted every 30 min with a 1- or 2-point rolling window (30-min or 1-h) smoothing function applied to the visualizations but not to values used for statistical analysis. $^*p < 0.05$, $^{**}p < 0.01$, $^{***}p < 0.001$, $^{****}p < 0.0001$ indicate statistical significance calculated by one-way ANOVA and two-way ANOVA followed by Tukey multiple comparison test. The illustration was created with BioRender.

See also Figure S2.

Please cite this article in press as: Fanti et al., Methionine-supplemented longevity diet increases growth hormone, GLP-1, and FGF21; reduces frailty; and promotes healthspan, Cell Metabolism (2026), https://doi.org/10.1016/j.cmet.2026.05.015

(Figures 2O, 2P, and S2L). This behavior was especially pronounced in females (Figures S2Q–S2T). Our results show that 23-month-old HET3 mice were able to lose and regain weight and modify RER levels as expected, even after 6 cycles of FMD. In the LDMM group, instead, after 3 months on the diet, we observed a slight decrease in EE consistent with their smaller size relative to controls.

Frailty and lifespan of HET3 mice in response to dietary interventions

To understand how different diets may affect function and strength in older HET3 mice, we measured the frailty index (FI) using the 31-item FI test[38] at 23 months (Figures 3A and S3A) and 26 months (Figures 3B and S3A). Additionally, muscle strength and motor coordination were assessed through grip strength and rotarod tests at 24 months (Figures 3C, 3D, and S2B–S2E). Female mice on the WD exhibited an earlier onset of frailty at 23 months compared with the SD ($p < 0.0001$), LDMM ($p = 0.001$), and FMD ($p = 0.007$) groups, and at 26 months, the WD-fed mice maintained the highest FI compared with all groups (Figure 3B). KD-fed mice had greater frailty than mice fed SD ($p = 0.006$) and LDMM ($p = 0.04$) at the same age. In 23-month-old males, FI was elevated in the WD and KD groups compared with the LDMM group ($p < 0.0001$ and $p = 0.003$) (Figure S3A). At 26 months, this trend persisted despite a less clear distinction between the diets, indicating that males experienced physiological decline earlier than females (Figure S3A). The findings on frailty align with those of motor coordination and muscle strength assessed at 24 months. In females, LDMM-fed mice showed the best performance on the rotarod, both in terms of absolute time to fall compared with WD ($p = 0.008$) and when adjusted for BW (time to fall/BW) in comparison to SD ($p = 0.01$), WD ($p = 0.001$), and KD ($p = 0.006$) (Figure 3C). There was no difference after adjustment for lean mass (Figure S3B), whereas LDMM males exhibited only a trend toward improved rotarod performance either in absolute time to fall or adjusted for BW and lean mass (Figure S3C).

Finally, there were no differences in absolute strength or strength adjusted for LBM (strength/LBM) among females (Figures 3D and S3D) and males (Figure S3E). However, when strength was adjusted for BW (strength/BW), LDMM exhibited superior grip strength performance compared with SD ($p = 0.006$), WD ($p < 0.0001$), and KD ($p < 0.0001$), in both females and males (Figures 3D and S3E). Grip strength in FMD group mice was also higher when compared with WD and KD in males (Figure S3E).

To assess the mechanisms underlying differences in frailty across dietary groups, we measured Pax7 protein expression in muscle after 5 months of dietary intervention. Pax7 is a transcriptional regulator crucial for the myogenic function of satellite cells and, as such, a marker of muscle regeneration and repair. Typically quiescent, these cells activate Pax7 in response to growth or injury, promoting the fusion of myogenic precursor cells with existing myofibers or the formation of new ones.[39] In our study, regardless of age, 10 cycles of FMD in 5 months resulted in a Pax7 increase 4 days after refeeding, suggesting a long-lasting activation of satellite cells in muscle (Figures 3E and S3F). This result may, in part, explain the preservation of muscle mass and function at least in the FMD group.

We also performed cognitive tests on female and male mice at 24 months of age. The Y-maze, novel object recognition, and Barnes maze tests revealed no significant differences between groups, suggesting that in old HET3 mice without any appreciable cognitive decline, 4 months of these nutritional interventions do not cause measurable effects on short- or long-term memory (Figures S3G–S3J).

The lifespan study provided a clearer picture of the long-term effects of diet. In males, no significant difference was found between groups (log-rank test, $p = 0.2$; Figure 3F). Conversely, the analysis in females indicated that one or more groups had a different survival probability (log-rank test, $p = 0.046$) (Figure 3G). In females, LDMM intervention starting at 20 months extended the median lifespan by 5.6% compared with WD ($p = 0.007$, Benjamini-Hochberg [BH] $p$adj = 0.05; Figures 3H and S3K) and 7.2% compared with FMD ($p = 0.01$; BH $p$adj = 0.05; Figures 3P and S3K). This effect is further supported by the 25% survival rate observed with LDMM, reflecting the efficacy of the intervention in delaying age-related mortality (Figure S3K). For females, this rate is 7% higher than that of SD (Figure S3L). Regarding maximum lifespan, in agreement with its effects on frailty and cardiometabolic markers, WD showed a major reduction of up to 200 days compared with the longest-lived SD and LDMM groups, −16% and −15%, respectively, in females and −9.7% and −8%, respectively, in males (Figure S3K). The lifespans observed with the KDs and FMDs fell in between, except for one female outlier in the KD group, which reached a maximum lifespan of 1,210 days (Figure S3K). These results align with previous data in C57BL/6J mice, showing positive effects of FMD cycles between 16 and 25 months, but not in very old mice, when deaths increased in the FMD group compared with controls.[40]

Additionally, a Cox proportional hazards (PHs) regression model was used to estimate relative risk, using the SD group as the reference (Figure S3L). The hazard ratio (HR) for all pairwise groups (if applicable) was greater than 1, except for the LDMM group, which was 0.94 and 0.95 for females and males, respectively. However, the observed 5%–6% reduction in mortality risk for the LDMM group was not statistically significant. Along with the Kaplan-Meier analysis showing minor differences in overall survival, we conclude that starting LDMM treatment at 20 months has a strong effect on healthspan but no significant effect on lifespan in both females and males when compared with the control SD treatment.

Finally, necropsies of HET3 mice that died from natural causes revealed that the incidence and type of neoplastic lesions varied based on dietary consumption (Figure S3M). The most common causes of death among HET3 mice include lymphoma, hemangiosarcoma, and lung carcinoma, which collectively account for 70% of cases.[41] In our study, necropsies of combined female and male mice fed a control diet (SD) throughout their lives revealed a neoplasia incidence proportion of approximately 66%, including both benign and malignant tumors (Figure S3M). The mice fed the KD showed a higher proportion of tumor incidence (74%), of which only 16% were benign (Figure S3M). Unlike the other groups, malignancy particularly affected the liver. Approximately 62% of WD mice developed tumors, of which 4.8% were benign. Notably, because WD mice have a reduced life expectancy, the incidence of tumors may be underestimated due to premature

Please cite this article in press as: Fanti et al., Methionine-supplemented longevity diet increases growth hormone, GLP-1, and FGF21; reduces frailty; and promotes healthspan, Cell Metabolism (2026), https://doi.org/10.1016/j.cmet.2026.05.015

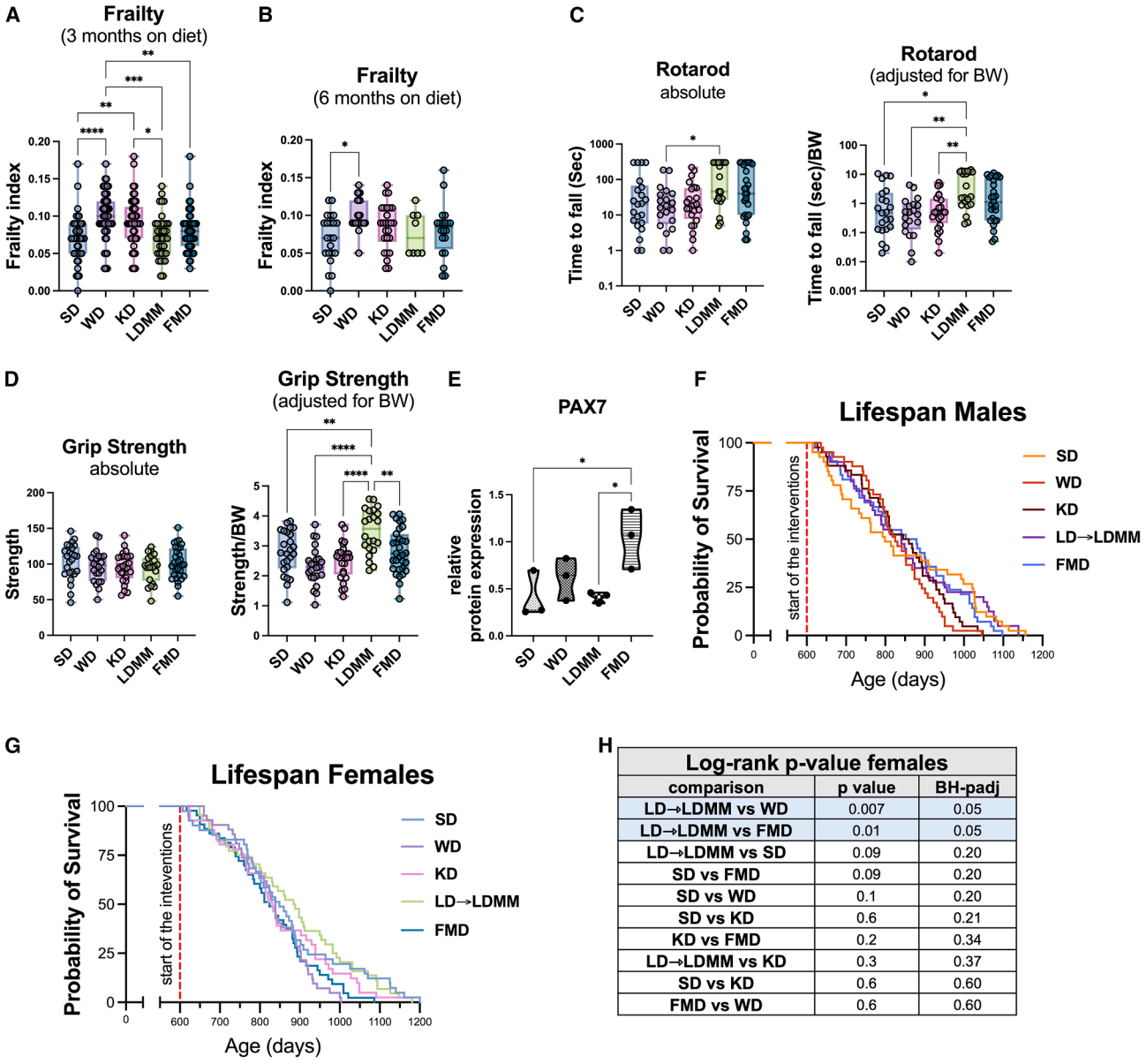

H

Log-rank p-value females		
comparison	p value	BH-padj
LD→LDMM vs WD	0.007	0.05
LD→LDMM vs FMD	0.01	0.05
LD→LDMM vs SD	0.09	0.20
SD vs FMD	0.09	0.20
SD vs WD	0.1	0.20
SD vs KD	0.6	0.21
KD vs FMD	0.2	0.34
LD→LDMM vs KD	0.3	0.37
SD vs KD	0.6	0.60
FMD vs WD	0.6	0.60

Figure 3. Effects of nutritional interventions on the frailty and lifespan of HET3 mice

(A and B) FI was assessed in females at 23 (n = 38–51/group) and 26 (n = 8–26/group) months of age.

(C) Rotarod was performed on female mice after 4 months on the diets. The data show absolute (time to fall/s) and adjusted for BW (time to fall/BW). y axis is presented on a $\log_{10}$ scale (n = 20–27/group).

(D) Grip strength was performed on female HET3 mice after 4 months on the diets. The data show absolute strength and strength adjusted for BW (strength/BW) (n = 22–31/group).

(E) Densitometry analysis of Pax7 (30 mg of quadriceps/sample; n = 3 mice/group).

(F–H) Kaplan-Meier survival curves for male and female HET3 mice were plotted separately; differences among diet groups within each sex were tested using the log-rank test (n = 41–44/group). The table displays pairwise comparisons of median lifespan. The Benjamini-Hochberg (BH) correction was applied to adjust for multiple testing.

(A–G) Mice in the LDMM group received LD for 1–2 weeks before switching to the LDMM.

Data are presented as mean ± SEM. *p < 0.05, **p < 0.01, ***p < 0.001, ****p < 0.0001 indicate statistical significance calculated by one-way ANOVA followed by Tukey multiple comparison test or using Kruskal-Wallis test followed by Dunn's multiple comparisons test.

See also Figure S3.

Please cite this article in press as: Fanti et al., Methionine-supplemented longevity diet increases growth hormone, GLP-1, and FGF21; reduces frailty; and promotes healthspan, Cell Metabolism (2026), https://doi.org/10.1016/j.cmet.2026.05.015

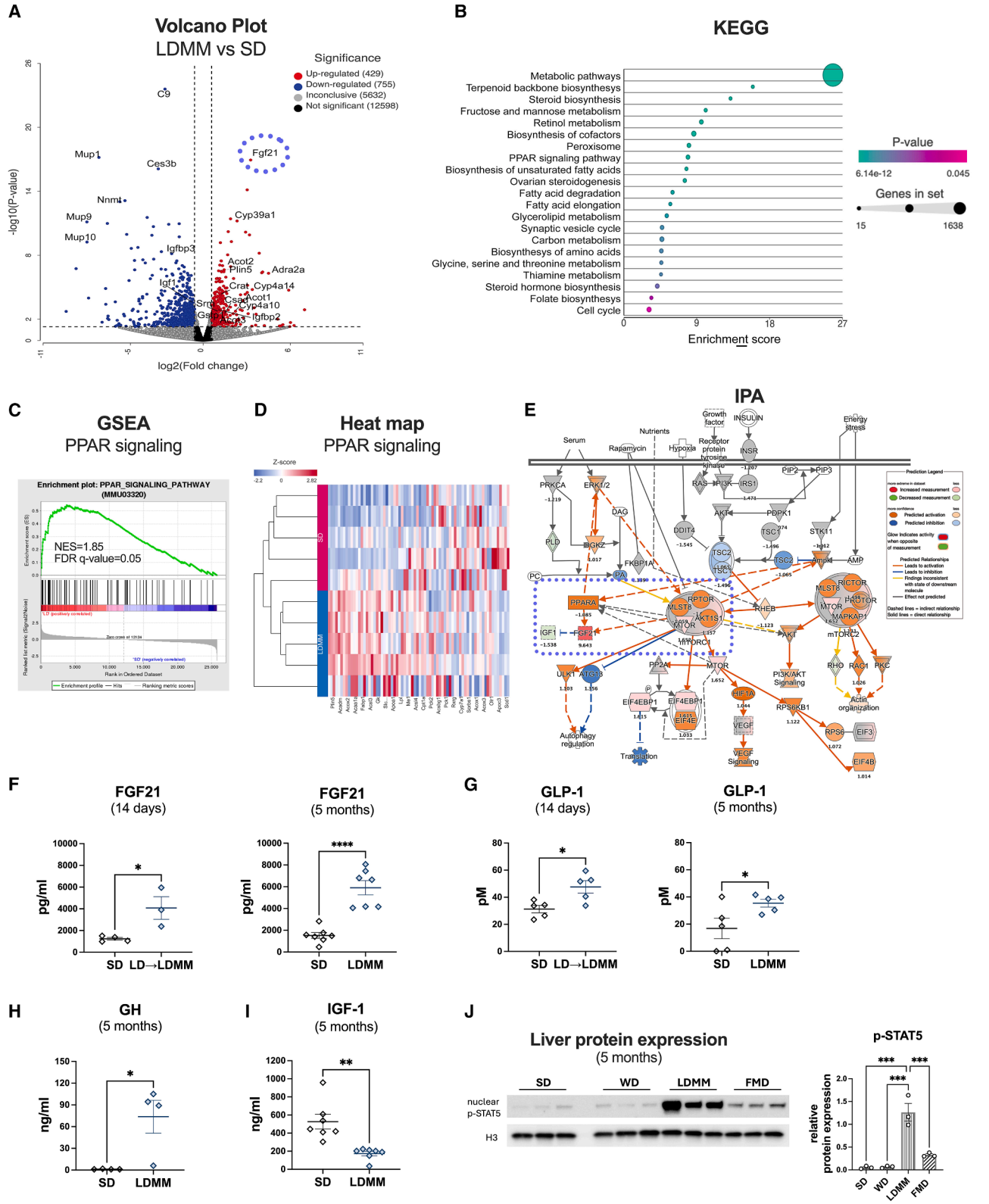

Figure 4. RNA-seq reveals elevated *Fgf21* expression and genes associated with longevity in the liver of female HET3 mice

(A) Volcano plot of DEG in LDMM versus SD (n = 5/group). The x axis represents $\log_2$(fold change), the y axis represents −log10(p value). Downregulated genes are represented in blue, while upregulated genes are represented in red.

(legend continued on next page)

Please cite this article in press as: Fanti et al., Methionine-supplemented longevity diet increases growth hormone, GLP-1, and FGF21; reduces frailty; and promotes healthspan, Cell Metabolism (2026), https://doi.org/10.1016/j.cmet.2026.05.015

death from other causes, likely heart and kidney failure. The LDMM and FMD groups had the lowest tumor counts, at 57% and 56%, respectively, indicating that the healthspan effects of both diets may be partially attributed to the prevention of age-related diseases, including cancer.

RNA-seq data reveal high expression of FGF21 and other longevity-associated genes in the liver of HET3 mice

We then focused on the LDMM, which had the strongest effects on promoting overall health and longevity in older mice compared with other diets.

As the liver regulates systemic glucose levels, growth factors, and lipids in response to nutritional status, we analyzed liver gene expression in 25-month-old female HET3 mice fed for 5 months with either the LDMM or SD (n = 5/group) to gain insights into the molecular mechanisms mediating the effects of the LDMM. Principal-component analysis (PCA) revealed that the two dietary groups cluster separately, mostly along PC1/PC2/PC3, indicating a shift in overall gene expression profiles between SD and LDMM groups (Figure S4A). Differential gene expression (DGE) analysis identified 429 upregulated and 755 downregulated genes in LDMM compared with SD (Figure 4A; $p < 0.05$ and FC > 1.5 or <−1.5). Most significantly, upregulated genes in LDMM were involved in metabolic processes. Among them was *Fgf21* (FC = 9.64, p = 1.16e−17), *Adra2A*, and other fatty acid metabolism genes, such as *Acot1*, *Acot2*, and *Acot3*, and *Tsku*, a hepatokine that responds to increased thermogenesis and EE.[42] TSKU acts as a hormonal feedback mechanism that reduces energy use after an initial phase of increased EE, promoting metabolic adaptation and weight maintenance.

In line with other pro-longevity interventions,[43] we noted several upregulated genes in glutathione metabolism, including *Gstp1* and *Gstt2*, as well as in PPAR signaling, including *Cyp4a10*, *Cyp4a14*, *Fabp1*, *Plin4*, and *Plin5*, along with their downstream targets, *Ucp2* and *Crat*. Several genes associated with lifespan extension and involved in methionine/cysteine metabolism were also found to be differentially upregulated, including *Srm* and *Csad*, which have been linked to spermidine[44] and taurine[45] production, whereas methyltransferase genes *Nnmt* and *Bhmt* were downregulated. Similarly, various major urinary protein (MUP) genes, found to be downregulated in GH-deficient mouse models,[43] and *Ces3b*, a carboxylesterase implicated in hepatic lipid regulation,[46] were also downregulated. Moreover, LDMM induced significant transcriptional changes in *Igf-1* and *Igf*-binding proteins, critical modulators of insulin-like growth factor (IGF)-1 activity. Specifically, *Igf-1* and *Igfbp3* were downregulated, whereas *Igfbp2* was upregulated. Gene Ontology (GO) analysis of upregulated genes (FC > 2) (Figures S4B–S4D) revealed significant enrichment of biological processes, molecular functions, and cellular components associated with lipid metabolism, including cholesterol, small molecules, and alcohol metabolic processes; supported by findings from Kyoto Encyclopedia of Genes and Genomes (KEGG) showing significant enrichment primarily in metabolic pathways, including PPAR signaling, fatty acid metabolism, carbon metabolism, and biosynthesis of amino acids (Figure 4B). Underrepresented pathways (KEGG, based on differentially expressed genes [DEGs] with FC < −2) were instead associated with, among others, protein digestion and absorption, transforming growth factor β (TGF-β) signaling, and sulfur metabolism (Figure S4F).

Gene set enrichment analysis (GSEA) also highlighted enrichment of PPAR signaling (Figure 4C; NES = 1.85). A heatmap of the PPAR signaling pathway reveals hierarchical clustering of the SD and LDMM samples, indicating a substantial shift in gene expression (Figure 4D).

Finally, ingenuity pathway analysis (IPA) of the DEGs in LDMM versus SD revealed predicted activation of several pathways involved in cholesterol metabolism, including the mevalonate pathway and PPARα-mediated lipid metabolism regulation (Figure S4G). The analysis predicted potential direct interactions between PPARα and fibroblast growth factor (FGF)21, as well as indirect interactions between mechanistic target of rapamycin (mTOR) and FGF21, suggesting that the LDMM may modulate liver metabolic reprogramming through complex signaling crosstalk in which FGF21 plays a key role (Figure 4E).

LD increases FGF21 and GLP-1 and has differential effects on GH and IGF-1 in 25-month-old HET3 mice

Next, we measured specific circulating markers that may explain the beneficial cardiometabolic effects of the LDMM in 25-month-old female HET3 mice after 5 months of intervention. Consistent with hepatic transcriptome data, we confirmed that FGF21 was increased in the serum of LDMM mice ($p < 0.0001$) (Figure 4F). FGF21 is a circulating protein primarily produced by the liver to maintain metabolic homeostasis in response to nutritional stress,[47,48] including amino acid starvation,[49] such as methionine restriction,[50,51] and is implicated in longevity extension in rodents.[48] Analysis of the samples collected after 14 days of

(B) Kyoto Encyclopedia of Genes and Genomes (KEGG) enriched pathways in LDMM versus SD. Pathways are ranked by enrichment score (x axis). Color indicates the p value ($p < 0.05$), and size indicates the number of genes in each gene set.
(C) Enrichment plot of PPAR signaling pathway from the gene set enrichment analysis (GSEA) between LDMM and SD.
(D) Heatmap of gene expression in the PPAR signaling pathway showing hierarchical clustering of the samples from LDMM and SD.
(E) IPA predicts a crosstalk regulation between mTOR, PPARα, and FGF21 in response to the LD. Schematic representation of the mTOR pathway derived from IPA of DEGs in LDMM versus SD, including connection to PPARα and FGF21. Upregulated genes are shown in red, downregulated genes are shown in green. Predicted activation (orange) or inhibition (blue) of molecules, based on DGE, are also shown. Fold change in gene expression for detected genes is shown below each molecule.
(F–I) Circulating levels of FGF21 (F) and GLP-1 (G) after 14 days and 5 months of diets (n = 3–7/group) as well as GH (H) and IGF-1 (I) after 5 months of diets (n = 4–7/group).
(J) Western blot and densitometry analysis of hepatic nuclear phosphorylation of STAT5 after 5 months of diet (n = 3/group).
Mice in the LDMM group in the 5-month intervention received LD for 1–2 weeks before switching to the LDMM. Data are presented as mean ± SEM. *$p < 0.05$, **$p < 0.01$, ***$p < 0.001$, ****$p < 0.0001$ indicate statistical significance calculated by Student's unpaired t test and one-way ANOVA followed by Tukey multiple comparison test.
See also Figure S4.

Please cite this article in press as: Fanti et al., Methionine-supplemented longevity diet increases growth hormone, GLP-1, and FGF21; reduces frailty; and promotes healthspan, Cell Metabolism (2026), https://doi.org/10.1016/j.cmet.2026.05.015

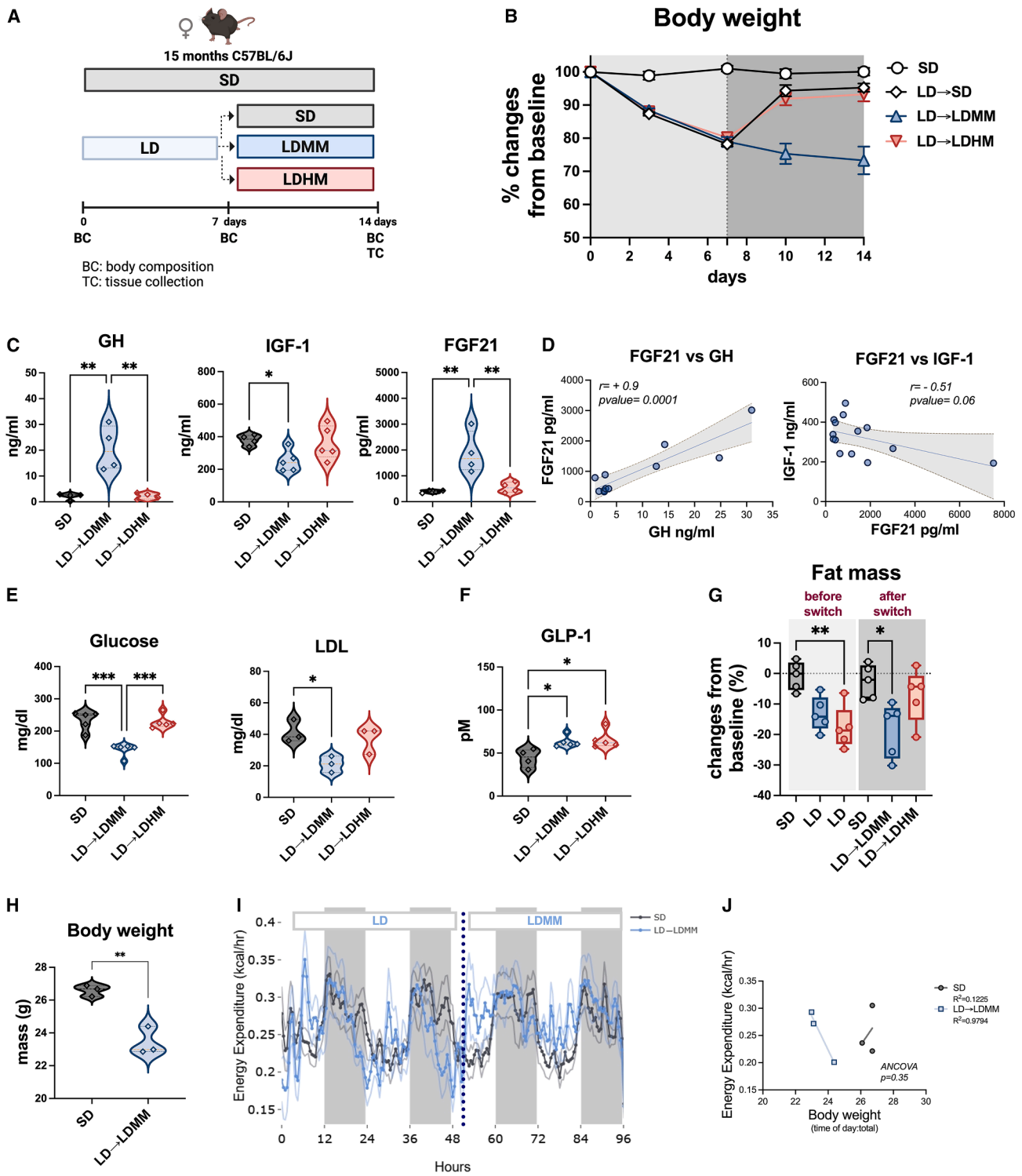

Figure 5. Supplementing methionine to match levels in the control diet reverses the effects of the LD in female C57BL/6J mice

(A) Overview of the experimental design involving 15-month-old female C57BL/6J wild-type (WT) mice (n = 4–5/group). The mice were fed LD (methionine 0.14%) for 7 days before being switched to SD (methionine 0.7%), LDMM (methionine 0.3%), or LDHM (0.7%). Body composition was assessed at baseline, before switching, and at the end of the experiment.

(B) Changes in BW.

(C) Circulating FGF21, GH, and IGF-1.

(legend continued on next page)

Please cite this article in press as: Fanti et al., Methionine-supplemented longevity diet increases growth hormone, GLP-1, and FGF21; reduces frailty; and promotes healthspan, Cell Metabolism (2026), https://doi.org/10.1016/j.cmet.2026.05.015

LDMM shows that FGF21 production increased early ($p = 0.02$) and remained sustained throughout the dietary intervention (Figure 4F). Also, levels of GLP-1, an insulinotropic incretin that controls glucose and adiposity,[52] were elevated after 14 days ($p = 0.01$) and after 5 months ($p = 0.05$) of intervention (Figure 4G), implying a possible link with FGF21. Surprisingly, GH levels were high ($p = 0.02$) (Figure 4H), whereas IGF-1 levels were low ($p = 0.001$), in the serum of LDMM mice (Figure 4I).

Based on our findings, we tested the hypothesis that FGF21 overexpression inhibits IGF-1 transcription by repressing STAT5.[53] Although transcriptome data indicate reduced *Igf-1* expression, surprisingly, liver protein analysis measured after 5 months of dietary intervention in female HET3 mice showed a 24-fold increase in nuclear-phosphorylated STAT5 (p-STAT5) in LDMM compared with SD, a 19-fold increase compared with WD but only an ~4-fold change compared with FMD (Figures 4J and S4H). These results suggest a strong activation of the liver GH receptor and its downstream target STAT5, which, instead of inducing the expression of target genes such as IGF-1[54] to promote growth, shifts toward the transcriptional regulation of hepatic genes involved in STAT5-dependent metabolic processes.[55] It has been shown that overactivation of GH-STAT5 suppresses lipogenic gene expression, such as *Scd-1*, likely through indirect mechanisms.[56] Accordingly, in the liver of LDMM mice, *Scd-1* was downregulated.

Methionine supplementation to match its levels in the SD reverses LD effects in C57BL/6J mice

We tested the hypothesis that methionine levels modulate the effects of LD in a short-term experiment in 15-month-old female C57BL/6J wild-type (WT) mice ($n = 4–5$/group), one of the genetic backgrounds represented in HET3 mice. The intervention began with LD administration until the mice achieved a mean weight loss of 20%. As anticipated, after 7 days on LD, when the limiting BW loss was reached, the mice were switched to (1) SD (0.7% methionine), (2) LDMM (0.3% methionine, otherwise identical to LD), or (3) LDHM (0.7% methionine, otherwise identical to LD) (Table S2) for 7 additional days before tissue collection. Body composition was measured at baseline, before the diet switch, and at the end of the study (Figure 5A). Consistent with the larger/longer study using HET3 mice, supplementation with moderate methionine (LDMM) stabilized BW (Figure 5B) and increased GH and FGF21 (Figure 5C). Conversely, supplementation with higher methionine levels, matching those in SD (LDHM), completely reversed the effect of LD on BW (Figure 5B). Circulating FGF21 and GH also decreased, while IGF-1 increased, indicating that high methionine levels have opposite effects on GH/FGF21 and IGF-1 release (Figure 5C). Accordingly, FGF21 showed strong positive and negative correlations with circulating GH and IGF-1 levels, respectively (Pearson correlation, GH, $r = +0.9$, $p = 0.0001$; IGF-1, $r = -0.51$, $p = 0.06$) (Figures 5D and S5A). Glycemia and LDL returned to baseline levels (Figures 5E and S5C), implying that glucose and LDL levels are also regulated by dietary methionine, although methionine supplementation did not significantly affect HDL levels (Figure S5B). As observed in HET3 mice (Figure 4G), GLP-1 was increased in the WT mice after 7 days of LDMM (Figure 5F). A trend for an increase in glucagon (Figure S5D) was also observed in a similar experiment conducted on 12-month-old female C57BL/6J mice using the same protocol (Figure 5A), except that LD was administered for 9 days. Methionine supplementation to 0.7% (LDHM) did not lower GLP-1 but prevented fat loss (Figure 5G) and decreased glucagon to basal levels (Figure S5D). These results support the conclusion that specific dietary methionine concentration, in an otherwise low-amino-acid diet, increases GH, GLP-1, FGF-21, and potentially glucagon, while allowing IGF-1 and LDL levels to remain relatively low.

To determine whether the rapid weight and fat loss caused by the LDMM (Figure 5G) was caused by increased heat production, as observed in studies reducing methionine levels in the diet,[57] we measured EE in 12-month-old female C57BL/6J mice fed the LD → LDMM and compared them with SD-fed controls. Data were collected over 180 h, including the transition from LD to LDMM. Although LD → LDMM mice exhibited reduced BW (Figure 5H), along with a trend of increased EE, the overall EE in LDMM mice was comparable to that of controls (Figures 5I and S5E) after adjustment for body mass (Figure 5J), indicating that increased EE is not the main cause of weight loss. Notably, a limitation of this experiment is the small sample size ($n = 3$/group), pointing to the need for additional experiments to confirm these results.

FGF21 mediates the metabolic effects of the LD

Our RNA sequencing (RNA-seq) data indicated that *Fgf21* is highly expressed in LDMM-fed HET3 mice, a finding supported by increased circulating Fgf21 levels in both HET3 and C57BL/6J mice. To evaluate the role of FGF21 in weight loss and metabolism induced by the LDMM, we performed a short-term experiment, as previously described, using 6-month-old female FGF21KO mice (Figure S6A) and WT mice. The mice were fed

(D) Scatterplots visualizing the correlation between circulating levels of FGF21 versus GH and FGF21 versus IGF-1. Pearson's r and *p* value of the correlations are indicated.

(E and F) (E) Glucose, LDL ($n = 3–5$/group), and (F) GLP-1 in circulation.

(G) Changes in fat mass (% from baseline).

(H and I) (H) BW and (I) plot of EE versus time (EE, kcal/h) measured in 12-month-old female WT mice ($n = 3$/group) fed LD (0.14% methionine) for 9 days before switching to LDMM (0.3% methionine) for 7 more days (gray bars indicate dark photoperiods). The figure shows the time plot of the data over 96 h during the transition from LD to LDMM. The complete 180-h measurement is shown in Figure S5E. Data versus time is plotted as group means for each diet ± SEM, represented by the line and ribbon, respectively. Data are plotted every 30 min, with a 3-point rolling window (90 min) smoothing function applied to the visualizations but not to values used in statistical analysis.

(J) ANCOVA for EE, with body mass as covariate, shows no significant difference between the SD and LD → LDMM groups. A mass × diet interaction effect was not significant.

Data are presented as means ± SEM. $^{*}p < 0.05$, $^{**}p < 0.01$, $^{***}p < 0.001$ indicate statistical significance calculated by one-way ANOVA followed by Tukey multiple comparison test and Student's unpaired *t* test. The illustration was created with BioRender.

See also Figure S5.

Please cite this article in press as: Fanti et al., Methionine-supplemented longevity diet increases growth hormone, GLP-1, and FGF21; reduces frailty; and promotes healthspan, Cell Metabolism (2026), https://doi.org/10.1016/j.cmet.2026.05.015

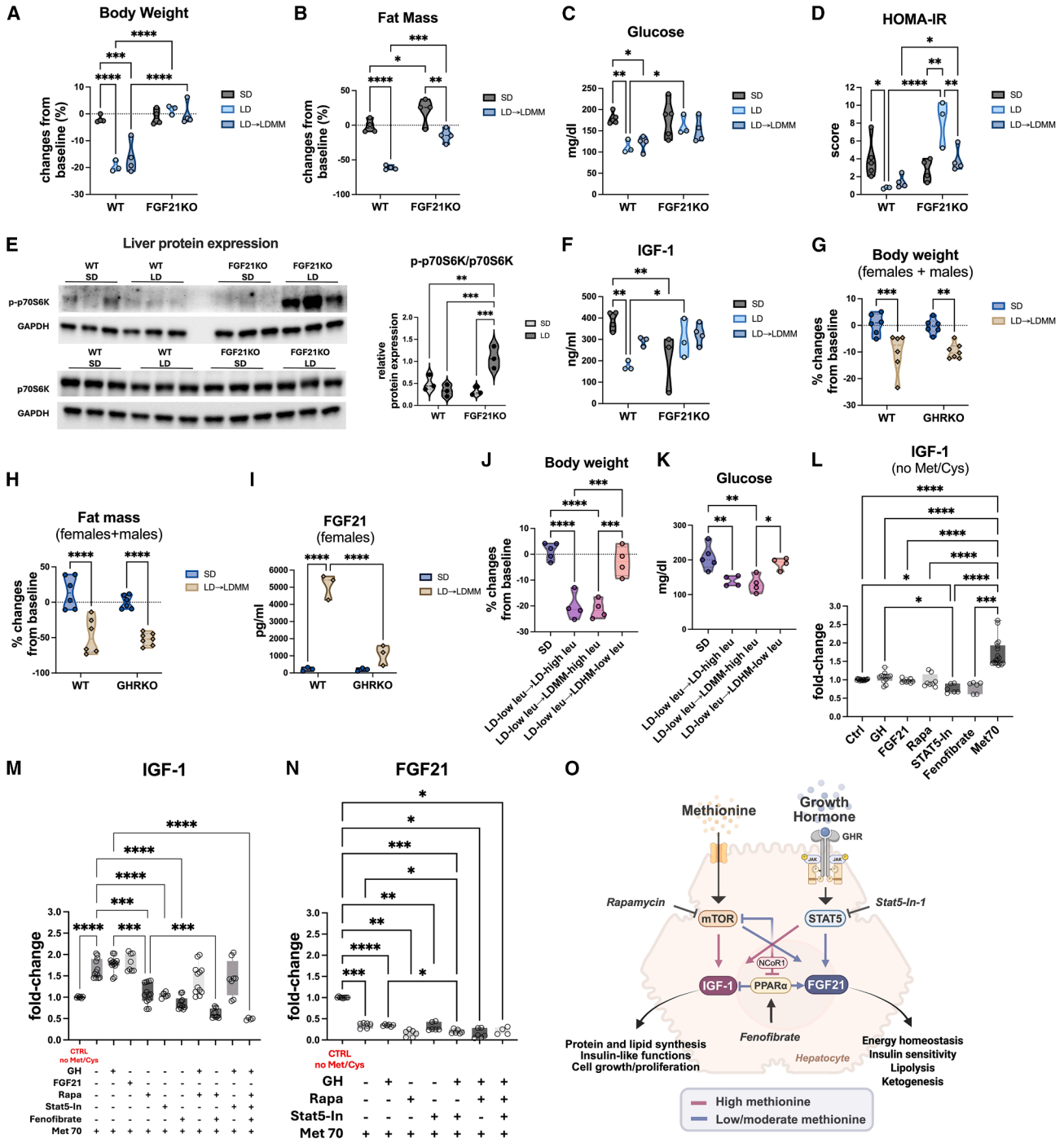

Figure 6. Methionine-dependent regulation of hepatic mTOR-PPARα crosstalk underlies the metabolic benefits of the LD by coordinating FGF21 and IGF-1 release

Experiment 1: 6-month-old female WT and FGF21KO mice (n = 4/group) were fed LD (methionine 0.14%) for 7 days before switching to LDMM (methionine 0.3%) for an additional 5 days. A separate group was fed LD for 12 days (n = 3 mice/strain). Body composition was assessed at baseline, before the diet switch, and at the end of the experiment. Experiment 2: 9-month-old female and male WT and GHRKO mice (n = 6/group) were fed LD for 7 days, then switched to a moderate-methionine diet for an additional 7 days. Experiment 3: 12-month-old female WT mice (n = 4/group) were fed LD (LM-low leu: 0.14% methionine and 0.71% leucine) for 7 days before switching to an LD with (1) low methionine and high leucine (LM-high leu: 0.14% methionine and 1.5% leucine), (2) moderate methionine and high leucine (LDMM-high leu: 0.3% methionine and 1.5% leucine), or (3) high methionine and low leucine (HM-low leu: 0.7% methionine and 0.71% leucine).

(A) Changes in body weight (BW) (%) from baseline (experiment 1).

(B) Changes in fat mass (%) from baseline (experiment 1).

(C) Fasting glucose (experiment 1).

(legend continued on next page)

Please cite this article in press as: Fanti et al., Methionine-supplemented longevity diet increases growth hormone, GLP-1, and FGF21; reduces frailty; and promotes healthspan, Cell Metabolism (2026), https://doi.org/10.1016/j.cmet.2026.05.015

the LD for 7 days before transitioning to the LDMM for an additional 5 days. A separate group was maintained on the LD throughout the entire experiment. As expected, WT mice responded to LD and LD → LDMM by reducing BW by ∼20% ($p < 0.0001$) and ∼18% ($p = 0.0001$) (Figure 6A), respectively. The fat mass decreased by ∼60% ($p < 0.0001$) at the end of the LD → LDMM intervention (Figure 6B). In contrast, FGF21KO mice did not display weight loss in response to either LD or LD → LDMM (Figure 6A), although a slight reduction in fat mass (∼10%, $p = 0.001$) was observed (Figure 6B). FGF21KO mice, which typically exhibit a higher liver-to-BW ratio than WT mice,[58] did not show a reduction in liver size, likely reflecting an inability to decrease liver fat accumulation in response to LD → LDMM (Figure S6B). Instead, lean mass remained unchanged except for a single FGF21-deficient mouse (Figure S6C). In addition, in FGF21KO mice on LD → LDMM, serum glucose levels did not decrease under either LD or LD → LDMM (Figure 6C) despite a major increase in insulin levels (Figure S6D), indicating an insulin-resistant phenotype. This is also supported by the significant increase in the HOMA-IR score (Figure 6D) along with increased hepatic p-p70S6K/S6K (Figure 6E) and p-AKT/AKT protein levels (Figures S6E and S6F) measured after 12 days of continuous LD. FGF21 also negatively regulated IGF-1 levels/availability during the LD → LDMM feeding (Figure 6F). IGF-1 levels in FGF21KO control mice were lower than in WT control mice, which explains the smaller size observed at baseline compared with WT mice (Figure S6G). Interestingly, FGF21KO mice exhibited a trend toward increased IGF-1 levels in response to LD and LD → LDMM, although these changes were not statistically significant (Figure 6F). Together, these results show that both LD and LDMM regulate fat, glucose, and insulin levels/sensitivity through an FGF21-dependent mechanism.

LD's effects are in part dependent on GH-STAT5 contribution to FGF21 production

The increased GH and reduced IGF-1 levels in mice fed the LDMM led us to evaluate the role of GH signaling in mediating the effects of the LD. We performed a short-term experiment, as previously described, on 9-month-old female and male GHR-deficient (GHRKO) mice and age-matched WT controls. GHRKO mice exhibit very low IGF-1 and high GH levels/signaling. The low IGF-1 levels contribute to dwarfism in these mice, which grow extremely slowly and remain significantly smaller than WT mice.[59] Unlike FGF21KO mice, the effects of LD → LDMM on BW (Figure 6G), fat mass (Figure 6H), lean mass (Figure S6H), and glucose (Figure S6I) in GHRKO mice were not different from those of WT mice, except that in the GHRKO mice, there was no reduction in liver fat accumulation (Figure S6J). Additionally, FGF21 levels were significantly lower in the GHRKO mice than in the WT mice on LD → LDMM ($p < 0.0001$) (Figure 6I), suggesting that GH signaling does not control weight loss but regulates FGF21 production in mice subjected to moderate methionine conditions, presumably under the control of p-STAT5, as seen in both HET3 (Figure 4L) and, to a milder extent, C57BL/6J (Figures S5F and S5G), after either long-term or short-term treatments, respectively. Interestingly, while LD → LDMM required GH (GHRKO) to increase FGF21 levels, it did not require FGF21 (FGF21KO) to increase GH (Figure S6K).

Leucine concentration matching the control diet does not reverse the effects of the LD

We also investigated whether restricting leucine, an essential amino acid that replicates some of the benefits of methionine restriction,[60,61] mimics the effects of methionine modulation on body composition. In a short-term experiment, 12-month-old female WT mice were fed LD, which is low in methionine and leucine (0.14% methionine, 0.71% leucine), for 7 days, then switched to (1) LD supplemented with high leucine to match levels of the control SD (LD-high leu: 0.14% methionine, 1.5% leucine), (2) LD supplemented with moderate methionine and high leucine (LDMM-high leu: 0.3% methionine, 1.5% leucine), or (3) LD supplemented only with high methionine (LDHM-low leu: 0.7% methionine, 0.71% leucine) for 7 additional days (Table S2). Only LDHM-low leu, with methionine levels matching

(D) HOMA-IR (experiment 1).
(E) Western blot and densitometry of liver protein p-p70S6K(Thr389)/p70S6K expression (experiment 1).
(F) Circulating IGF-1 (experiment 1).
(G) Changes in BW (%) (experiment 2).
(H) Changes from baseline in fat mass (%) (experiment 2).
(I) Circulating FGF21 (experiment 2).
(J) Changes in BW (%) (experiment 3).
(K) Fasting glucose (experiment 3).
(L) IGF-1 measured in conditioned media of primary mouse hepatocytes, cultured in methionine/cysteine- and FBS-free media, in response to methionine supplementation (70 μg/L), GH (500 ng/mL), FGF21 (250 ng/mL), rapamycin (100 nM), STAT5-In-1 inhibitor (100 μM), and fenofibrate (400 μM) (biological replicates $n = 3–7$).
(M) IGF-1 measured in conditioned media of primary mouse hepatocytes, cultured in methionine/cysteine- and FBS-free media and supplemented with methionine (70 μg/L), in response to GH (500 ng/mL), FGF21 (250 ng/mL), rapamycin (100 nM), STAT5-In-1 (100 μM), and fenofibrate (400 μM) (biological replicates $n = 2–5$).
(N) FGF21 measured in conditioned media of primary mouse hepatocytes, cultured in methionine/cysteine- and FBS-free media and supplemented with methionine (70 μg/L), in response to GH (500 ng/mL), rapamycin (100 nM), and STAT5-In-1 (100 μM) (biological replicates $n = 2$).
(O) The diagram illustrates how methionine levels modulate the interaction among mTOR, GH/STAT5, and PPARα in hepatocytes, thereby affecting the release of FGF21 and IGF-1 by the liver.
Data are presented as means ± SEM. $*p < 0.05$, $**p < 0.01$, $***p < 0.001$, $****p < 0.0001$ indicate statistical significance calculated by one-way ANOVA followed by Tukey multiple comparison test or one-way ANOVA with Welch's one-way followed by Games-Howell multiple comparisons test.
See also Figure S6.

Please cite this article in press as: Fanti et al., Methionine-supplemented longevity diet increases growth hormone, GLP-1, and FGF21; reduces frailty; and promotes healthspan, Cell Metabolism (2026), https://doi.org/10.1016/j.cmet.2026.05.015

those of the SD, reversed BW, serum glucose (Figures 6J and 6K), and fat mass (Figure S6L). Notably, leucine levels in LD and LDMM mice are half of those in the SD group, whereas methionine is 5 times lower in the LD group and about 2.5 times lower in the LDMM group compared with the SD cohort (Table S2). Future studies will investigate the role of leucine and other amino acids in mediating the effects of LD.

Methionine levels modulate hepatic mTOR-PPARα crosstalk, regulating IGF-1 and FGF21 release

Liver protein analysis showed PPARα upregulation in C57BL/6J mice after 12 days of LD administration (*t* test: $p = 0.05$) (Figure S6M). We also observed a non-significant trend of increased PPARα in C57BL/6J after 14 days of LD → LDMM. This effect is partially reversed in LDHM (Figures S5F and S2G). Furthermore, RNA-seq of liver from HET3 mice after 5 months of LDMM revealed upregulation of several PPARα target genes, including FGF21,[62] as well as predicted interactions between mTOR, FGF21, and PPARα (Figure 4E).

The mTORC1 regulates hepatic homeostasis and inhibits ketogenesis through the repressive activity of S6K2, which recruits nuclear receptor corepressor 1 (NCoR1) and represses the PPARα transcription factor.[63,64] On the contrary, S6K2 deficiency enhances PPARα.[63] Adult C57BL/6J mice given short-term LDMM or LDHM show increased and decreased ketone body production, respectively (Figure S5C). This supports the hypothesis that low/moderate methionine levels promote fat catabolism and ketogenesis, while high levels inhibit these processes. Given that SAMTOR acts as a SAM sensor that connects methionine to mTORC1 signaling,[65] FGF21 has been shown to inhibit mTORC1,[66] and FGF21-deficient mice exhibit significant insulin-stimulated mTORC1 activation and worsening hepatic IR,[66] we hypothesize that dietary methionine levels in LDMM regulate hepatic homeostasis via a crosstalk between the SAMTOR-mTOR and PPARα-FGF21 pathways.

First, we measured NCoR1 liver protein in C57BL/6J mice fed LD → LDMM and LD → HM (Figure 5A). Consistent with our hypothesis, NCoR1 decreased in LD → LDMM-fed mice but returned to control levels in LD → LDHM-fed mice (Figure S6N). Second, we evaluated the effect of methionine on IGF-1 and FGF21 release from primary mouse hepatocytes grown in DMEM without methionine, cysteine, and fetal bovine serum (FBS). Experiments on hepatocytes using culture media restricted only in methionine showed intermediate effects on metabolic parameters (MTS assay) compared with the more potent effects observed with media restricted in both methionine and cysteine (data not shown). In fact, cysteine supplementation is known to counteract the effects of methionine restriction *in vivo*, highlighting the crucial role of methionine as a cysteine precursor and the compensatory role of cysteine in MetR conditions.[31,67] Because our focus was on the role of methionine in cellular processes, to avoid confounding factors, we used culture media limited to both amino acids to detect even minor effects on IGF-1 and FGF21 release induced by methionine supplementation.

The hepatocytes were, therefore, treated with media supplemented with (1) a range of methionine levels for dose-response evaluation; (2) a single dose of methionine; (3) GH; (4) rapamycin, an mTOR inhibitor; (5) STAT5-In-1, a STAT5 inhibitor; (6) FGF21; and (7) fenofibrate, a PPARα agonist. Combinations of treatments were also tested.

The analysis of conditioned media from primary hepatocytes in response to varying methionine concentrations demonstrated a positive correlation with IGF-1 release and a negative correlation with FGF21 release (Figure S6O). Based on these results, we identified 70 μg/L as the "high" methionine dose that promotes IGF-1 release and FGF21 inhibition (Figure S6O). Total protein analysis indicated changes in p-p70S6K/p70S6K in hepatocytes treated with GH, rapamycin, and the combination of GH + rapamycin, with or without 70 μg/L methionine, thus confirming the methionine-dependent activation of the mTOR pathway (Figure S6P). Further analysis showed that methionine is required for IGF-1 synthesis and release (Figure 6L) and that inhibition of mTOR by rapamycin blocks IGF-1 production/release in response to methionine (Figure 6M; all *p* values in Table S3). Despite the presence of rapamycin, GH continued to increase IGF-1 levels, indicating that GH does not regulate IGF-1 in an mTOR-dependent manner. Instead, GH failed to increase IGF-1 levels in a medium lacking methionine/cysteine (Figure 6L), suggesting that methionine is crucial for the GH-dependent IGF-1 synthesis/release by the liver. In the methionine-enriched medium, while STAT5-In inhibited IGF-1, GH + STAT5 inhibition partially restored IGF-1 levels (Figure 6M; all *p* values in Table S3). The combination of the PPARα agonist fenofibrate with rapamycin inhibited IGF-1 release more than rapamycin alone, suggesting an additive effect of the two drugs (Figure 6M; all *p* values in Table S3). Conversely, the presence of methionine inhibits the release of FGF21 in primary hepatocytes (Figures 6N and S6Q). A non-significant trend of increased FGF21 levels was observed in response to fenofibrate, whereas STAT5 or mTOR inhibition reduced FGF21 release in primary hepatocytes, regardless of methionine concentration in the medium (Figures 6N and S6Q). These findings support the role of methionine levels in increasing IGF-1 expression while reducing FGF21 expression. They also support the hypothesis that GH-STAT5-mTOR signaling upregulates FGF21 under methionine-deficient conditions but upregulates IGF-1 expression when methionine levels are sufficiently high (Figure 6O). Although these *in vitro* results are generally consistent with the *in vivo* data, additional *in vivo* studies will be necessary to confirm our hypotheses on the underlying mechanisms.

Re-interpretation of epidemiological data on protein consumption and obesity/diabetes risk

Malik et al.[68] analyzed the association between total, animal, and plant-based protein intake and the incidence of T2D in 72,992 women from the Nurses' Health Study (NHS, 1984–2008), 92,088 women from the Nurses' Health Study II (NHSII, 1991–2009), and 40,722 men from the Health Professionals Follow-up Study (HPFS, 1986–2008). They found that the highest quintiles of total and animal protein intake were associated with 39% and 49% higher risk of T2D compared with the lowest quintiles, which decreased to 7% and 13%, respectively, after adjusting for BMI. In contrast, relatively higher intake of plant-based protein was associated with a moderately lower risk of T2D.

Here, we reanalyzed the data from these studies, taking into account the results from the mouse studies. Cross-sectional associations between lifestyle and cardiometabolic risk factors by

Please cite this article in press as: Fanti et al., Methionine-supplemented longevity diet increases growth hormone, GLP-1, and FGF21; reduces frailty; and promotes healthspan, Cell Metabolism (2026), https://doi.org/10.1016/j.cmet.2026.05.015

Table 1. Risk factors according to quintile of animal and plant-based protein in the NHS, NHSII, and HPFS

NHS-NHSII-HPFS	Animal protein intake				NHS-NHSII-HPFS	Plant-based protein intake			
Characteristics	Q1	Q5	% difference	*p* value	Characteristics	Q1	Q5	% difference	*p* value
Median total protein (% kcal/day)	13.68	21.34	+56.01	N/A	median total protein (% kcal/day)	16.83	17.45	+3.67	N/A
Median animal protein (% kcal/day)	7.69	16.07	+108.97	N/A	median plant protein (% kcal/day)	4.11	7.29	+77.37	N/A
Methionine (g/day)	1.27	2.30	+81.47	<0.001	methionine (g/day)	1.80	1.69	−6.44	<0.001
Total energy (kcal/day)	1,853.97	1,677.91	−9.50	<0.001	total energy (kcal/day)	1,865.25	1,734.22	−7.02	<0.001
Alcohol use (g/day)	6.35	4.11	−35.17	<0.001	alcohol use (g/day)	7.15	4.05	−43.37	<0.001
Sugar-sweetened beverages (serv/day)	0.60	0.16	−73.75	<0.001	sugar-sweetened beverages (serv/day)	0.78	0.13	−83.04	<0.001
Prevalence of BMI (kg/m^2) >25 (%)	45.27	60.60	+33.86	<0.001	prevalence of BMI (kg/m^2) >25 (%)	56.92	46.65	−18.04	<0.001
Prevalence of T2D (%)	3.95	8.11	+105.32	<0.001	prevalence of T2D (%)	4.18	6.93	+65.79	<0.001
Prevalence of high cholesterol (%)	44.57	43.29	−2.87	<0.001	prevalence of high cholesterol (%)	40.56	45.04	+11.05	<0.001
Prevalence of hypertension (%)	30.68	31.48	+2.61	0.01	prevalence of hypertension (%)	30.20	29.33	−2.88	0.01

Data are presented as means for continuous variables and percentages for categorical variables. When comparing quintile 5 to quintile 1, *p* values were calculated using *t* tests for continuous variables and χ^2 tests for categorical variables. Percent of energy from protein (kcal/day) was estimated by multiplying grams of protein consumed per day by the number of kcal in 1 gram of protein (4 kcal/g) and dividing by total caloric intake. Analyses were conducted at the midpoint of follow-up: 1998 for the NHS, 1999 for NHSII, and 1998 for HPFS.See also Table S4–S6.

quintile of animal and plant protein intake were examined using data from the midway of follow-up: 1998, 1999, and 1998 for the NHS, NHSII, and HPFS, respectively (Table 1). Notably, individuals in the highest compared with the lowest quintile of animal protein intake (+109%) were also more likely to exhibit habits consistent with a healthier lifestyle, including lower calorie intake (−9.5%), lower alcohol consumption (−35.17%), and much lower intake of sugar-sweetened beverages (−73.75%) (Tables 1 and S4). They also displayed a slightly lower prevalence of high cholesterol (−2.87%) (all $p < 0.001$ for comparison of extreme quintiles) (Tables 1 and S5). At the same time, those in the highest compared with the lowest quintile of animal protein intake were more likely to be in an overweight/obesity range (+34%) and to have T2D (+105.82%) and hypertension (+2.61%) (all $p < 0.01$) (Tables 1 and S5). Conversely, individuals in the highest quintile of plant-based protein intake were less likely to have overweight/obesity (−18.04%) and hypertension (−2.88%) ($p < 0.01$). However, the risk of diabetes remained 65% higher than in the lowest quintile but was down from the 105% increase in the high-animal-protein group. Although the interpretation of these findings is complicated by the cross-sectional nature of the data, we analyzed the data to test the hypothesis that intake levels of specific amino acids, rather than protein intake itself, might be responsible for these counterintuitive results. In fact, we found that methionine intake was 81.47% higher in the top compared with the bottom quintile of animal protein intake ($p < 0.001$) but 6.44% lower in the top compared with the bottom quintile of plant-based protein intake ($p < 0.001$) (Tables 1 and S6). Similar trends were noted for lysine. The delta% in amino acid intake differences between animal and plant-based quintiles 1–5 was among the highest for methionine (+81.47 to −6.44) compared with any other amino acid, second only to lysine (+88.73 to −8.30). Although these results do not demonstrate that methionine is responsible for the associations between high-animal-protein intake and overweight/obesity or diabetes, together with our mouse data, they suggest that the high content of methionine and other essential amino acids in animal but not plant proteins could contribute to these conditions.

DISCUSSION

Traditional diets of long-lived populations, such as those of Japan and Southern Europe, are characterized by low levels of animal protein. In contrast, higher animal protein intake is prevalent in modern diets in the US and North-Central Europe and, more recently, in Southern Europe, partly due to the misconception that a high-protein diet is healthy and important for preventing muscle loss and frailty.[69]

Among the dietary patterns tested in old HET3 mice, we found that the WD, high in animal protein and fat, was, as expected, detrimental to health and longevity. The high-animal-protein KD, made with healthy foods including nuts and olive oil, had similar harmful effects. When compared with the healthy control SD alone, both FMD cycles and the methionine-supplemented LD, LDMM, improved a range of metabolic markers and healthspan but not lifespan. However, because the most effective pro-longevity interventions, including MetR, protein restriction, and calorie restriction[15,27,70] have reduced efficacy in extending lifespan when initiated late in life[26,71] it will be important to test

Please cite this article in press as: Fanti et al., Methionine-supplemented longevity diet increases growth hormone, GLP-1, and FGF21; reduces frailty; and promotes healthspan, Cell Metabolism (2026), https://doi.org/10.1016/j.cmet.2026.05.015

LDMM starting at a much younger age to assess its potential to extend lifespan.[72]

These results in mice could partly explain findings from three large epidemiological studies showing that participants consuming the highest levels of animal protein and therefore methionine and other essential amino acids, despite a lower calorie intake and healthy choices, had a higher prevalence of overweight/obesity and a doubling of the prevalence of diabetes compared with those consuming the least animal protein. In contrast, participants with the highest intake of plant protein, but a lower methionine intake, had a lower prevalence of overweight/obesity. The prevalence of diabetes was still higher than in those who ate the least amount of plant-based protein, but the increase was attenuated compared with the low- and high-animal-protein intake groups (Table 1). Notably, this cross-sectional analysis was not adjusted for health and lifestyle factors. In contrast, in the previously published cohort analysis of the same groups, diabetes risk was reduced rather than increased in the quintile with the highest plant protein intake but with an estimated lower methionine intake.[68]

One potential interpretation of the results is that the very high levels of methionine and essential amino acids in the high-animal-protein group are promoting both weight gain and diabetes. In fact, in the previous cohort study, adjustment for BMI eliminated most of the effects of a high-protein diet on the risk of T2D.[68] Accordingly, a recent pilot study showed that restricting sulfur amino acids, limiting both methionine and cysteine, promoted weight loss in humans.[73]

The LD was designed based on the diets traditionally followed by populations known for record life expectancies, such as those in Italy and Japan. However, the eating habits in these areas have changed over the past decades. In 1949, the typical protein intake in Okinawa was reported to be about 39 g, primarily from plant sources.[10] Similarly, lower-class southern Italians had limited access to animal-based products at the beginning of the 20th century due in part to the strict enforcement of national self-sufficiency policies in food production by the fascist regime.[74] As a result, legumes became an important source of protein from the 1920s to the 1960s. Because the methionine content per 100 g of legumes and other plant-based proteins is much lower than that found in most animal-based sources, high legume and low meat consumption is likely to have contributed to lower methionine and amino acid intake.[75] Therefore, many older Japanese and Italians have followed diets low in meat consumption during the earlier part of their lives, resulting in much lower levels of many amino acids, particularly essential amino acids such as methionine, followed by periods of increased protein intake starting in the 1960s and continuing into the later part of their lives.[76] The percentages of energy from carbohydrates/fat/protein in the LD without methionine supplementation (59/30/12) are similar to those estimated for the traditional Mediterranean diet (48/38/14)[77]and the modern Japanese diet (56/28/15),[78] but not for the modern diet in Italy (46/37/17),[79–81] particularly for protein intake. However, the very low levels of methionine and other amino acids in traditional diets may also have contributed to greater frailty among elderly populations in Southern Europe[21] and Japan.[82]

Notably, the methionine/cysteine content in LDMM, which provides half the amino acid levels of the control diet and which is much higher than that in the MetR diets[29] used in lifespan studies,[27] appears to be required to prevent frailty in mice fed an LD.

These results are consistent with previous studies in *Drosophila*, in which adding methionine to an amino acid-restricted diet restored fecundity without abolishing the longevity benefit, indicating that a specific amino acid profile can promote both lifespan and healthspan.[83]

The hepatic transcriptome of LDMM overlaps with that of long-lived mice, including GH- or GHR-deficient mice, FGF21-overexpressing mice, and methionine restriction models,[43] and is associated with activation of crucial metabolic pathways, including PPAR signaling and *Fgf21* activity, an essential mediator of the MetR diet.[50] According to our *in vivo* and *in vitro* results, the most plausible model is that, in the liver, high GH levels activate STAT5 and mTOR, thereby increasing IGF-1 production only when methionine levels are sufficiently high. However, if methionine availability is limited, PPARα is activated, and IGF-1 levels decrease. Under these conditions, GH-STAT5-mTOR signaling also promotes hepatic FGF21 production (Figure 6O).

GLP-1, increased under LDMM, was not sensitive to changes in dietary methionine concentration, which were clearly responsible for regulating fat mass and IR. Notably, previous studies have shown that Liraglutide, a GLP-1RA, does not cause weight loss in FGF21KO mice,[84] raising the possibility that, in our study, GLP-1 may act by regulating FGF21 in response to the LDMM. Notably, whereas GLP-1 treatment in humans is associated with decreased appetite, fat loss, and lean mass loss,[3] LDMM-fed mice consumed high levels of calories and food and lost fat mass without losing lean body mass, pointing to the need to test the effect of LDMM in humans.

In conclusion, we propose that the LDMM achieves a range of healthspan-promoting effects, in part by increasing GH, GLP-1, and FGF21 while limiting IGF-1 levels. High dietary methionine levels, and possibly those of other amino acids, could help explain part of the association between a diet rich in animal proteins, overweight/obesity, diabetes, and high mortality in humans. Finally, because both high and low levels of one or a few amino acids can make such a remarkable difference, this study suggests that recommendations for protein intake should be complemented by those for personalized amino acid profile intake.

Limitations of the study

A major limitation of the lifespan study was that the experiment started very late in life, at 20 months of age, when the efficacy of dietary interventions is known to be limited. Beginning treatment earlier in life could potentially lead to stronger effects of LDMM on lifespan. Regarding the re-analysis of the epidemiological data, although changes in reported methionine consumption are consistent with weight gain/loss and diabetes incidence, we cannot conclude that methionine is causing weight gain or promoting diabetes in these human studies.

RESOURCE AVAILABILITY

Lead contact

Requests for further information and resources should be directed to and will be fulfilled by the lead contact, Valter D. Longo (vlongo@usc.edu).

Materials availability

This study did not generate any new or unique reagents.

Data and code availability

Data used for the graphs and full lists of differentially abundant transcripts are available in Data S1, the source data table. Raw and processed bulk RNA-seq data files have been deposited in NCBI's Gene Expression Omnibus (GEO: GSE297351). This article does not report original code. Data analysis is described in the STAR Methods section of this article, and additional information required to reanalyze the data is available from the lead contact upon request.

ACKNOWLEDGMENTS

This work was funded by NIH and NIA grants (GR1045540 and AG084485) and the USC Edna Jones Chair Fund. We acknowledge the assistance of the Integrative Liver Cell Core (ILCC) at the Southern California Research Center for ALPD and Cirrhosis (5 R24AA012885). We also thank Chayanne Schloffman for her contributions to mouse colony maintenance.

AUTHOR CONTRIBUTIONS

Conceptualization, M.F. and V.D.L.; methodology, M.F.; investigation, M.F., S.B., T.E.M., G.N., G.G., A.D., G.C.A., and D.C.; epidemiological analysis, V.S.M. and F.B.H.; RNA-seq analysis, L.P. and V.V.; performance and interpretation of mouse autopsies, L.D.; writing – original draft, M.F. and V.D.L.; all authors have read, reviewed, and approved the final manuscript.

DECLARATION OF INTERESTS

V.D.L. has equity interest in L-Nutra, a company that develops medical foods. V.D.L., T.E.M., and S.B. have filed patents related to the FMD at the University of Southern California. The University of Southern California has licensed its intellectual property to L-Nutra. As part of this license agreement, the University has the potential to receive royalty payments from L-Nutra.

V.D.L. and M.F. are inventors on a US provisional patent application filed by the University of Southern California that covers aspects of the methods and findings described in this manuscript.

STAR★METHODS

Detailed methods are provided in the online version of this paper and include the following:

- KEY RESOURCES TABLE
- EXPERIMENTAL MODEL AND STUDY PARTICIPANT DETAILS
  - Mice
  - Primary mouse hepatocytes
- METHOD DETAILS
  - Healthspan and longevity studies
  - Mechanistic studies
  - Dietary interventions
  - Food intake, body weight, and body composition assessment
  - Indirect calorimetry analysis
  - Frailty Index Assessment
  - Glucose Tolerance Test (GTT) and Insulin Tolerance Test (ITT)
  - Circulating markers
  - Novel Object Recognition Test
  - Barnes Maze
  - Y-Maze
  - Grip Strength
  - Rotarod
  - Protein analysis
  - RNA extraction, sequencing, and data analysis
  - *In vitro* experiment
  - Epidemiological data
- QUANTIFICATION AND STATISTICAL ANALYSIS

SUPPLEMENTAL INFORMATION

Supplemental information can be found online at https://doi.org/10.1016/j.cmet.2026.05.015.

Received: May 20, 2025
Revised: December 4, 2025
Accepted: May 29, 2026

REFERENCES

1. Meier, J.J. (2012). GLP-1 receptor agonists for individualized treatment of type 2 diabetes mellitus. Nat. Rev. Endocrinol. *8*, 728–742. https://doi.org/10.1038/nrendo.2012.140.
2. Hathaway, J.T., Shah, M.P., Hathaway, D.B., Zekavat, S.M., Krasniqi, D., Gittinger, J.W., Cestari, D., Mallery, R., Abbasi, B., Bouffard, M., et al. (2024). Risk of nonarteritic anterior ischemic optic neuropathy in patients prescribed semaglutide. JAMA Ophthalmol. *142*, 732–739. https://doi.org/10.1001/jamaophthalmol.2024.2296.
3. Linge, J., Birkenfeld, A.L., and Neeland, I.J. (2024). Muscle mass and glucagon-like peptide-1 receptor agonists: adaptive or maladaptive response to weight loss? Circulation *150*, 1288–1298. https://doi.org/10.1161/CIRCULATIONAHA.124.067676.
4. Xie, Y., Choi, T., and Al-Aly, Z. (2025). Mapping the effectiveness and risks of GLP-1 receptor agonists. Nat. Med. *31*, 951–962. https://doi.org/10.1038/s41591-024-03412-w.
5. Shetty, R., Basheer, F.T., Poojari, P.G., Thunga, G., Chandran, V.P., and Acharya, L.D. (2022). Adverse drug reactions of GLP-1 agonists: A systematic review of case reports. Diabetes Metab. Syndr. *16*, 102427. https://doi.org/10.1016/j.dsx.2022.102427.
6. Budini, B., Luo, S., Tam, M., Stead, I., Lee, A., Akrami, A., Vidal-Puig, A., and Park, A. (2026). Trajectory of weight regain after cessation of GLP-1 receptor agonists: a systematic review and nonlinear meta-regression. EClinicalMedicine *93*, 103796. https://doi.org/10.1016/j.eclinm.2026.103796.
7. WHO (2024). Life Expectancy At Birth (Years) – Indicator Details (Global Health Observatory: World Health Organization).
8. Foreman, K.J., Marquez, N., Dolgert, A., Fukutaki, K., Fullman, N., McGaughey, M., Pletcher, M.A., Smith, A.E., Tang, K., Yuan, C.W., et al. (2018). Forecasting life expectancy, years of life lost, and all-cause and cause-specific mortality for 250 causes of death: reference and alternative scenarios for 2016–40 for 195 countries and territories. Lancet *392*, 2052–2090. https://doi.org/10.1016/S0140-6736(18)31694-5.
9. Tsugane, S. (2020). Why has Japan become the world's most long-lived country: insights from a food and nutrition perspective. Eur. J. Clin. Nutr. *75*, 921–928. https://doi.org/10.1038/s41430-020-0677-5.
10. Willcox, B.J., Willcox, D.C., Todoriki, H., Fujiyoshi, A., Yano, K., He, Q., Curb, J.D., and Suzuki, M. (2007). Caloric restriction, the traditional Okinawan diet, and healthy aging: The diet of the world's longest-lived people and its potential impact on morbidity and life span. Ann. N. Y. Acad. Sci. *1114*, 434–455. https://doi.org/10.1196/annals.1396.037.
11. Longo, V.D., and Anderson, R.M. (2022). Nutrition, longevity and disease: From molecular mechanisms to interventions. Cell *185*, 1455–1470. https://doi.org/10.1016/j.cell.2022.04.002.
12. Bamia, C., Trichopoulos, D., Ferrari, P., Overvad, K., Bjerregaard, L., Tjønneland, A., Halkjaer, J., Clavel-Chapelon, F., Kesse, E., Boutron-Ruault, M.C., et al. (2007). Dietary patterns and survival of older Europeans: The EPIC-Elderly Study (European Prospective Investigation into Cancer and Nutrition). Public Health Nutr. *10*, 590–598. https://doi.org/10.1017/S1368980007382487.
13. Willett, W.C., Sacks, F., Trichopoulou, A., Drescher, G., Ferro-Luzzi, A., Helsing, E., and Trichopoulos, D. (1995). Mediterranean diet pyramid: a cultural model for healthy eating. Am. J. Clin. Nutr. *61*, 1402S–1406S. https://doi.org/10.1093/ajcn/61.6.1402S.

14. Hyun, D.H., Emerson, S.S., Jo, D.G., Mattson, M.P., and de Cabo, R. (2006). Calorie restriction up-regulates the plasma membrane redox system in brain cells and suppresses oxidative stress during aging. Proc. Natl. Acad. Sci. USA *103*, 19908–19912. https://doi.org/10.1073/pnas.0608008103.

15. Anderson, R.M., Shanmuganayagam, D., and Weindruch, R. (2009). Caloric restriction and aging: studies in mice and monkeys. Toxicol. Pathol. *37*, 47–51. https://doi.org/10.1177/0192623308329476.

16. Das, J.K., Banskota, N., Candia, J., Griswold, M.E., Orenduff, M., de Cabo, R., Corcoran, D.L., Das, S.K., De, S., Huffman, K.M., et al. (2023). Calorie restriction modulates the transcription of genes related to stress response and longevity in human muscle: The CALERIE study. Aging Cell *22*, e13963. https://doi.org/10.1111/acel.13963.

17. Aversa, Z., White, T.A., Heeren, A.A., Hulshizer, C.A., Saul, D., Zhang, X., Molina, A.J.A., Redman, L.M., Martin, C.K., Racette, S.B., et al. (2023). Calorie restriction reduces biomarkers of cellular senescence in humans. Aging Cell *23*, e14038. https://doi.org/10.1111/acel.14038.

18. Obeid, C.A., Gubbels, J.S., Jaalouk, D., Kremers, S.P.J., and Oenema, A. (2022). Adherence to the Mediterranean diet among adults in Mediterranean countries: a systematic literature review. Eur. J. Nutr. *61*, 3327–3344. https://doi.org/10.1007/s00394-022-02885-0.

19. León-Muñoz, L.M., Guallar-Castillón, P., Graciani, A., López-García, E., Mesas, A.E., Aguilera, M.T., Banegas, J.R., and Rodríguez-Artalejo, F. (2012). Adherence to the Mediterranean diet pattern has declined in Spanish adults. J. Nutr. *142*, 1843–1850. https://doi.org/10.3945/jn.112.164616.

20. Tong, T.Y.N., Appleby, P.N., Armstrong, M.E.G., Fensom, G.K., Knuppel, A., Papier, K., Perez-Cornago, A., Travis, R.C., and Key, T.J. (2020). Vegetarian and vegan diets and risks of total and site-specific fractures: results from the prospective EPIC-Oxford study. BMC Med. *18*, 353. https://doi.org/10.1186/s12916-020-01815-3.

21. O'Donovan, M.R., Devleesschauwer, B., Sezgin, D., Liew, A., Kabir, Z., and O'Caoimh, R. (2023). Comparing frailty prevalence between countries: validation of the Global Burden of Disease study Frailty Index (GBD-FI) in the survey of health, ageing and retirement in Europe. Age Ageing *52*, afad214. https://doi.org/10.1093/ageing/afad214.

22. Harrison, D.E., Strong, R., Sharp, Z.D., Nelson, J.F., Astle, C.M., Flurkey, K., Nadon, N.L., Wilkinson, J.E., Frenkel, K., Carter, C.S., et al. (2009). Rapamycin fed late in life extends lifespan in genetically heterogeneous mice. Nature *460*, 392–395. https://doi.org/10.1038/nature08221.

23. Kang, J., Benjamin, D.I., Kim, S., Salvi, J.S., Dhaliwal, G., Lam, R., Goshayeshi, A., Brett, J.O., Liu, L., and Rando, T.A. (2024). Depletion of SAM leading to loss of heterochromatin drives muscle stem cell ageing. Nat. Metab. *6*, 153–168. https://doi.org/10.1038/s42255-023-00955-z.

24. Lin, K., Wei, L., Wang, R., Li, L., Song, S., Wang, F., He, M., Pu, W., Wang, J., Wazir, J., et al. (2025). Disrupted methionine cycle triggers muscle atrophy in cancer cachexia through epigenetic regulation of REDD1. Cell Metab. *37*, 460–476.e8. https://doi.org/10.1016/j.cmet.2024.10.017.

25. Chaudhuri, R. (2025). The role of amino acids in skeletal muscle health and sarcopenia: A narrative review. J. Biomed. Res. *39*, 229–241. https://doi.org/10.7555/JBR.38.20240167.

26. Hernández-Arciga, U., Stamenkovic, C., Yadav, S., Nicoletti, C., Albalawy, W.N., Al Hammood, F., Gonzalez, T.F., Naikwadi, M.U., Graham, A., Smarz, C., et al. (2025). Dietary methionine restriction started late in life promotes healthy aging in a sex-specific manner. Sci. Adv. *11*, eads1532. https://doi.org/10.1126/sciadv.ads1532.

27. Miller, R.A., Buehner, G., Chang, Y., Harper, J.M., Sigler, R., and Smith-Wheelock, M. (2005). Methionine-deficient diet extends mouse lifespan, slows immune and lens aging, alters glucose, T4, IGF-I and insulin levels, and increases hepatocyte MIF levels and stress resistance. Aging Cell *4*, 119–125. https://doi.org/10.1111/j.1474-9726.2005.00152.x.

28. Orentreich, N., Matias, J.R., Defelice, A., and Zimmerman, J.A. (1993). Low methionine ingestion by rats extends life span. J. Nutr. *123*, 269–274. https://doi.org/10.1093/jn/123.2.269.

29. Forney, L.A., Wanders, D., Stone, K.P., Pierse, A., and Gettys, T.W. (2017). Concentration-dependent linkage of dietary methionine restriction to the components of its metabolic phenotype. Obesity (Silver Spring) *25*, 730–738. https://doi.org/10.1002/oby.21806.

30. Richie, J.P., Sinha, R., Dong, Z., Nichenametla, S.N., Ables, G.P., Ciccarella, A., Sinha, I., Calcagnotto, A.M., Chinchilli, V.M., Reinhart, L., et al. (2023). Dietary methionine and total sulfur amino acid restriction in healthy adults. J. Nutr. Health Aging *27*, 111–123. https://doi.org/10.1007/s12603-023-1883-3.

31. Lee, A.H., Orliaguet, L., Youm, Y.H., Maeda, R., Dlugos, T., Lei, Y., Coman, D., Shchukina, I., Andhey, P.S., Smith, S.R., et al. (2025). Cysteine depletion triggers adipose tissue thermogenesis and weight loss. Nat. Metab. *7*, 1204–1222. https://doi.org/10.1038/s42255-025-01297-8.

32. Lees, E.K., Król, E., Grant, L., Shearer, K., Wyse, C., Moncur, E., Bykowska, A.S., Mody, N., Gettys, T.W., and Delibegovic, M. (2014). Methionine restriction restores a younger metabolic phenotype in adult mice with alterations in fibroblast growth factor 21. Aging Cell *13*, 817–827. https://doi.org/10.1111/acel.12238.

33. Miller, R.A., Harper, J.M., Galecki, A., and Burke, D.T. (2002). Big mice die young: early life body weight predicts longevity in genetically heterogeneous mice. Aging Cell *1*, 22–29. https://doi.org/10.1046/j.1474-9728.2002.00006.x.

34. Valdemarin, F., Caffa, I., Persia, A., Cremonini, A.L., Ferrando, L., Tagliafico, L., Tagliafico, A., Guijarro, A., Carbone, F., Ministrini, S., et al. (2021). Safety and feasibility of fasting-mimicking diet and effects on nutritional status and circulating metabolic and inflammatory factors in cancer patients undergoing active treatment. Cancers *13*, 4013. https://doi.org/10.3390/cancers13164013.

35. Banks, A.S., Allison, D.B., Alquier, T., Ansarullah, Austad, S.N., Auwerx, J., Ayala, J.E., Baur, J.A., Carobbio, S., Churchill, G.A., et al. (2025). A consensus guide to preclinical indirect calorimetry experiments. Nat. Metab. *7*, 1765–1780. https://doi.org/10.1038/s42255-025-01360-4.

36. Mina, A.I., LeClair, R.A., LeClair, K.B., Cohen, D.E., Lantier, L., and Banks, A.S. (2018). CalR: a web-based analysis tool for indirect calorimetry experiments. Cell Metab. *28*, 656–666.e1. https://doi.org/10.1016/j.cmet.2018.06.019.

37. Tschöp, M.H., Speakman, J.R., Arch, J.R.S., Auwerx, J., Brüning, J.C., Chan, L., Eckel, R.H., Farese, R.V., Galgani, J.E., Hambly, C., et al. (2011). A guide to analysis of mouse energy metabolism. Nat. Methods *9*, 57–63. https://doi.org/10.1038/NMETH.1806.

38. Whitehead, J.C., Hildebrand, B.A., Sun, M., Rockwood, M.R., Rose, R.A., Rockwood, K., and Howlett, S.E. (2014). A clinical frailty index in aging mice: comparisons with frailty index data in humans. J. Gerontol. A Biol. Sci. Med. Sci. *69*, 621–632. https://doi.org/10.1093/gerona/glt136.

39. Sambasivan, R., Yao, R., Kissenpfennig, A., Van Wittenberghe, L., Paldi, A., Gayraud-Morel, B., Guenou, H., Malissen, B., Tajbakhsh, S., and Galy, A. (2011). Pax7-expressing satellite cells are indispensable for adult skeletal muscle regeneration. Development *138*, 3647–3656. https://doi.org/10.1242/dev.067587.

40. Brandhorst, S., Choi, I.Y., Wei, M., Cheng, C.W., Sedrakyan, S., Navarrete, G., Dubeau, L., Yap, L.P., Park, R., Vinciguerra, M., et al. (2015). A periodic diet that mimics fasting promotes multi-system regeneration, enhanced cognitive performance, and healthspan. Cell Metab. *22*, 86–99. https://doi.org/10.1016/j.cmet.2015.05.012.

41. Miller, R.A., Harrison, D.E., Astle, C.M., Baur, J.A., Boyd, A.R., de Cabo, R., Fernandez, E., Flurkey, K., Javors, M.A., Nelson, J.F., et al. (2011). Rapamycin, but not resveratrol or simvastatin, extends life span of genetically heterogeneous mice. J. Gerontol. A Biol. Sci. Med. Sci. *66*, 191–201. https://doi.org/10.1093/gerona/glq178.

42. Wang, Q., Sharma, V.P., Shen, H., Xiao, Y., Zhu, Q., Xiong, X., Guo, L., Jiang, L., Ohta, K., Li, S., et al. (2019). The hepatokine Tsukushi gates energy expenditure via brown fat sympathetic innervation. Nat. Metab. *1*, 251–260. https://doi.org/10.1038/s42255-018-0020-9.

43. Tyshkovskiy, A., Bozaykut, P., Borodinova, A.A., Gerashchenko, M.V., Ables, G.P., Garratt, M., Khaitovich, P., Clish, C.B., Miller, R.A., and

Gladyshev, V.N. (2019). Identification and application of gene expression signatures associated with lifespan extension. Cell Metab. *30*, 573–593. e8. https://doi.org/10.1016/j.cmet.2019.06.018.

44. Madeo, F., Eisenberg, T., Pietrocola, F., and Kroemer, G. (2018). Spermidine in health and disease. Science *359*, eaan2788. https://doi.org/10.1126/science.aan2788.
45. Singh, P., Gollapalli, K., Mangiola, S., Schranner, D., Yusuf, M.A., Chamoli, M., Shi, S.L., Lopes Bastos, B., Nair, T., Riermeier, A., et al. (2023). Taurine deficiency as a driver of aging. Science *380*, eabn9257. https://doi.org/10.1126/science.abn9257.
46. Lian, J., Wei, E., Groenendyk, J., Das, S.K., Hermansson, M., Li, L., Watts, R., Thiesen, A., Oudit, G.Y., Michalak, M., et al. (2016). Ces3/TGH deficiency attenuates steatohepatitis. Sci. Rep. *6*, 25747. https://doi.org/10.1038/srep25747.
47. Kharitonenkov, A., Shiyanova, T.L., Koester, A., Ford, A.M., Micanovic, R., Galbreath, E.J., Sandusky, G.E., Hammond, L.J., Moyers, J.S., Owens, R. A., et al. (2005). FGF-21 as a novel metabolic regulator. J. Clin. Invest. *115*, 1627–1635. https://doi.org/10.1172/JCI23606.
48. Hill, C.M., Albarado, D.C., Coco, L.G., Spann, R.A., Khan, M.S., Qualls-Creekmore, E., Burk, D.H., Burke, S.J., Collier, J.J., Yu, S., et al. (2022). FGF21 is required for protein restriction to extend lifespan and improve metabolic health in male mice. Nat. Commun. *13*, 1897. https://doi.org/10.1038/s41467-022-29499-8.
49. De Sousa-Coelho, A.L., Relat, J., Hondares, E., Pérez-Martí, A., Ribas, F., Villarroya, F., Marrero, P.F., and Haro, D. (2013). FGF21 mediates the lipid metabolism response to amino acid starvation. J. Lipid Res. *54*, 1786–1797. https://doi.org/10.1194/jlr.M033415.
50. Fang, H., Stone, K.P., Forney, L.A., Wanders, D., and Gettys, T.W. (2021). Nutritional regulation of hepatic FGF21 by dietary restriction of methionine. Front. Endocrinol. *12*, 773975. https://doi.org/10.3389/fendo.2021.773975.
51. Fang, H., Stone, K.P., Wanders, D., Forney, L.A., and Gettys, T.W. (2022). The origins, evolution, and future of dietary methionine restriction. Annu. Rev. Nutr. *42*, 201–226. https://doi.org/10.1146/annurev-nutr-062320-111849.
52. Müller, T.D., Finan, B., Bloom, S.R., D'Alessio, D., Drucker, D.J., Flatt, P. R., Fritsche, A., Gribble, F., Grill, H.J., Habener, J.F., et al. (2019). Glucagon-like peptide 1 (GLP-1). Mol. Metab. *30*, 72–130. https://doi.org/10.1016/j.molmet.2019.09.010.
53. Inagaki, T., Lin, V.Y., Goetz, R., Mohammadi, M., Mangelsdorf, D.J., and Kliewer, S.A. (2008). Inhibition of growth hormone signaling by the fasting-induced hormone FGF21. Cell Metab. *8*, 77–83. https://doi.org/10.1016/j.cmet.2008.05.006.
54. Rotwein, P. (2012). Mapping the growth hormone–Stat5b–IGF-I transcriptional circuit. Trends Endocrinol. Metab. *23*, 186–193. https://doi.org/10.1016/j.tem.2012.01.001.
55. Barclay, J.L., Nelson, C.N., Ishikawa, M., Murray, L.A., Kerr, L.M., McPhee, T.R., Powell, E.E., and Waters, M.J. (2011). GH-dependent STAT5 signaling plays an important role in hepatic lipid metabolism. Endocrinology *152*, 181–192. https://doi.org/10.1210/en.2010-0537.
56. Kaltenecker, D., Themanns, M., Mueller, K.M., Spirk, K., Suske, T., Merkel, O., Kenner, L., Luís, A., Kozlov, A., Haybaeck, J., et al. (2019). Hepatic growth hormone – JAK2 – STAT5 signalling: Metabolic function, non-alcoholic fatty liver disease and hepatocellular carcinoma progression. Cytokine *124*, 154569. https://doi.org/10.1016/j.cyto.2018.10.010.
57. Forney, L.A., Fang, H., Sims, L.C., Stone, K.P., Vincik, L.Y., Vick, A.M., Gibson, A.N., Burk, D.H., and Gettys, T.W. (2020). Dietary methionine restriction signals to the brain through fibroblast growth factor 21 to regulate energy balance and remodeling of adipose tissue. Obesity (Silver Spring) *28*, 1912–1921. https://doi.org/10.1002/oby.22919.
58. Fisher, F.M., Chui, P.C., Nasser, I.A., Popov, Y., Cunniff, J.C., Lundasen, T., Kharitonenkov, A., Schuppan, D., Flier, J.S., and Maratos-Flier, E. (2014). Fibroblast growth factor 21 limits lipotoxicity by promoting hepatic fatty acid activation in mice on methionine and choline-deficient diets. Gastroenterology *147*, 1073–1083.e6. https://doi.org/10.1053/j.gastro.2014.07.044.
59. Sun, L.Y., and Bartke, A. (2015). Tissue-specific GHR knockout mice: metabolic phenotypes. Front. Endocrinol. *5*, 243. https://doi.org/10.3389/fendo.2014.00243.
60. Lees, E.K., Banks, R., Cook, C., Hill, S., Morrice, N., Grant, L., Mody, N., and Delibegovic, M. (2017). Direct comparison of methionine restriction with leucine restriction on the metabolic health of C57BL/6J mice. Sci. Rep. *7*, 9977. https://doi.org/10.1038/s41598-017-10381-3.
61. Wanders, D., Stone, K.P., Dille, K., Simon, J., Pierse, A., and Gettys, T.W. (2015). Metabolic responses to dietary leucine restriction involve remodeling of adipose tissue and enhanced hepatic insulin signaling. BioFactors *41*, 391–402. https://doi.org/10.1002/biof.1240.
62. Inagaki, T., Dutchak, P., Zhao, G., Ding, X., Gautron, L., Parameswara, V., Li, Y., Goetz, R., Mohammadi, M., Esser, V., et al. (2007). Endocrine regulation of the fasting response by PPARalpha-mediated induction of fibroblast growth factor 21. Cell Metab. *5*, 415–425. https://doi.org/10.1016/j.cmet.2007.05.003.
63. Kim, K., Pyo, S., and Um, S.H. (2012). S6 kinase 2 deficiency enhances ketone body production and increases peroxisome proliferator-activated receptor alpha activity in the liver. Hepatology *55*, 1727–1737. https://doi.org/10.1002/hep.25537.
64. SenGupta, S., Peterson, T.R., Laplante, M., Oh, S., and Sabatini, D.M. (2010). mTORC1 controls fasting-induced ketogenesis and its modulation by ageing. Nature *468*, 1100–1104. https://doi.org/10.1038/nature09584.
65. Gu, X., Orozco, J.M., Saxton, R.A., Condon, K.J., Liu, G.Y., Krawczyk, P. A., Scaria, S.M., Harper, J.W., Gygi, S.P., and Sabatini, D.M. (2017). SAMTOR is an S-adenosylmethionine sensor for the mTORC1 pathway. Science *358*, 813–818. https://doi.org/10.1126/science.aao3265.
66. Gong, Q., Hu, Z., Zhang, F., Cui, A., Chen, X., Jiang, H., Gao, J., Chen, X., Han, Y., Liang, Q., et al. (2016). Fibroblast growth factor 21 improves hepatic insulin sensitivity by inhibiting mammalian target of rapamycin complex 1 in mice. Hepatology *64*, 425–438. https://doi.org/10.1002/hep.28523.
67. Stipanuk, M.H. (1986). Metabolism of sulfur-containing amino acids. Annu. Rev. Nutr. *6*, 179–209. https://doi.org/10.1146/annurev.nu.06.070186.001143.
68. Malik, V.S., Li, Y., Tobias, D.K., Pan, A., and Hu, F.B. (2016). Dietary protein intake and risk of type 2 diabetes in US men and women. Am. J. Epidemiol. *183*, 715–728. https://doi.org/10.1093/aje/kwv268.
69. International Food Information Council (2024). Food & health survey. https://ific.org/research/2024-food-health-survey/.
70. Fontana, L., Partridge, L., and Longo, V.D. (2010). Extending healthy life span—from yeast to humans. Science *328*, 321–326. https://doi.org/10.1126/science.1172539.
71. Hahn, O., Drews, L.F., Nguyen, A., Tatsuta, T., Gkioni, L., Hendrich, O., Zhang, Q., Langer, T., Pletcher, S., Wakelam, M.J.O., et al. (2019). A nutritional memory effect counteracts the benefits of dietary restriction in old mice. Nat. Metab. *1*, 1059–1073. https://doi.org/10.1038/s42255-019-0121-0.
72. Di Francesco, A., Deighan, A.G., Litichevskiy, L., Chen, Z., Luciano, A., Robinson, L., Garland, G., Donato, H., Vincent, M., Schott, W., et al. (2024). Dietary restriction impacts health and lifespan of genetically diverse mice. Nature *634*, 684–692. https://doi.org/10.1038/s41586-024-08026-3.
73. Olsen, T., Stolt, E., Øvrebø, B., Elshorbagy, A., Tore, E.C., Lee-Ødegård, S., Troensegaard, H., Johannessen, H., Doeland, B., Vo, A.A.D., et al. (2024). Dietary sulfur amino acid restriction in humans with overweight and obesity: a translational randomized controlled trial. J. Transl. Med. *22*, 40. https://doi.org/10.1186/s12967-023-04833-w.
74. Helstosky, C. (2004). Fascist food politics: Mussolini's policy of alimentary sovereignty. J. Mod. Ital. Stud. *9*, 1–26. https://doi.org/10.1080/1354571042000179164.
75. Gorissen, S.H.M., Crombag, J.J.R., Senden, J.M.G., Waterval, W.A.H., Bierau, J., Verdijk, L.B., and van Loon, L.J.C. (2018). Protein content and amino acid composition of commercially available plant-based

protein isolates. Amino Acids *50*, 1685–1695. https://doi.org/10.1007/s00726-018-2640-5.

76. Corrado, G. (2022). Food history and gastronomic traditions of beans in Italy. J. Ethn. Food *9*, 6. https://doi.org/10.1186/s42779-022-00122-x.
77. Menotti, A., and Puddu, P.E. (2025). Ancel Keys, the Mediterranean diet, and the Seven Countries Study: a review. J. Cardiovasc. Dev. Dis. *12*, 141. https://doi.org/10.3390/jcdd12040141.
78. Matsumura, Y. (2001). Nutrition trends in Japan. Asia Pac. J. Clin. Nutr. *10*, S40–S47. https://doi.org/10.1046/j.1440-6047.2001.00215.x.
79. Alberti-Fidanza, A., Fidanza, F., Chiuchiù, M.P., Verducci, G., and Fruttini, D. (1999). Dietary studies on two rural Italian population groups of the Seven Countries Study. 3. Trend of food and nutrient intake from 1960 to 1991. Eur. J. Clin. Nutr. *53*, 854–860. https://doi.org/10.1038/sj.ejcn.1600865.
80. Scarsi, N., Pastorino, R., Savoia, C., Raspolini, G.M., Pezzullo, A.M., and Boccia, S. (2025). Dietary patterns of adults in Italy: Results from the third Italian National Food Consumption Survey, INRAN-SCAI. PLoS One *20*, e0312977. https://doi.org/10.1371/journal.pone.0312977.
81. Mistura, L., Le Donne, C.L., D'Addezio, L., Ferrari, M., Comendador, F.J., Piccinelli, R., Martone, D., Sette, S., Catasta, G., Turrini, A., et al. (2025). The Italian IV SCAI dietary survey: Main results on food consumption. Nutr. Metab. Cardiovasc. Dis. *35*, 103863. https://doi.org/10.1016/j.numecd.2025.103863.
82. Kojima, G., Iliffe, S., Taniguchi, Y., Shimada, H., Rakugi, H., and Walters, K. (2017). Prevalence of frailty in Japan: A systematic review and meta-analysis. J. Epidemiol. *27*, 347–353. https://doi.org/10.1016/j.je.2016.09.008.
83. Grandison, R.C., Piper, M.D.W., and Partridge, L. (2009). Amino-acid imbalance explains extension of lifespan by dietary restriction in Drosophila. Nature *462*, 1061–1064. https://doi.org/10.1038/nature08619.
84. Le, T.D.V., Fathi, P., Watters, A.B., Ellis, B.J., Besing, G.K., Bozadjieva-Kramer, N., Perez, M.B., Sullivan, A.I., Rose, J.P., Baggio, L.L., et al. (2023). Fibroblast growth factor-21 is required for weight loss induced by the glucagon-like peptide-1 receptor agonist liraglutide in male mice fed high carbohydrate diets. Mol. Metab. *72*, 101718. https://doi.org/10.1016/j.molmet.2023.101718.
85. Schindelin, J., Arganda-Carreras, I., Frise, E., Kaynig, V., Longair, M., Pietzsch, T., Preibisch, S., Rueden, C., Saalfeld, S., Schmid, B., et al. (2012). Fiji: an open-source platform for biological-image analysis. Nat. Methods *9*, 676–682. https://doi.org/10.1038/NMETH.2019.
86. Charni-Natan, M., and Goldstein, I. (2020). Protocol for primary mouse hepatocyte isolation. STAR Protoc. *1*, 100086. https://doi.org/10.1016/j.xpro.2020.100086.
87. Trautman, M.E., Richardson, N.E., and Lamming, D.W. (2022). Protein restriction and branched-chain amino acid restriction promote geroprotective shifts in metabolism. Aging Cell *21*, e13626. https://doi.org/10.1111/acel.13626.
88. Levine, M.E., Suarez, J.A., Brandhorst, S., Balasubramanian, P., Cheng, C.W., Madia, F., Fontana, L., Mirisola, M.G., Guevara-Aguirre, J., Wan, J., et al. (2014). Low protein intake is associated with a major reduction in IGF-1, cancer, and overall mortality in the 65 and younger but not older population. Cell Metab. *19*, 407–417. https://doi.org/10.1016/j.cmet.2014.02.006.
89. Sinha, Y.N., Salocks, C.B., Wickes, M.A., and Vanderlaan, W.P. (1977). Serum and pituitary concentrations of prolactin and growth-hormone in mice during a twenty-four hour period. Endocrinology *100*, 786–791. https://doi.org/10.1210/endo-100-3-786.
90. Bellantuono, I., de Cabo, R., Ehninger, D., Di Germanio, C., Lawrie, A., Miller, J., Mitchell, S.J., Navas-Enamorado, I., Potter, P.K., Tchkonia, T., et al. (2020). A toolbox for the longitudinal assessment of healthspan in aging mice. Nat. Protoc. *15*, 540–574. https://doi.org/10.1038/s41596-019-0256-1.
91. Pitts, M.W. (2018). Barnes maze procedure for spatial learning and memory in mice. Bio-Protoc. *8*, e2744. https://doi.org/10.21769/BioProtoc.2744.
92. Fanti, M., Singh, S., Ledda-Columbano, G.M., Columbano, A., and Monga, S.P. (2014). Tri-iodothyronine induces hepatocyte proliferation by protein kinase A-dependent β-catenin activation in rodents. Hepatology *59*, 2309–2320. https://doi.org/10.1002/hep.26775.

Please cite this article in press as: Fanti et al., Methionine-supplemented longevity diet increases growth hormone, GLP-1, and FGF21; reduces frailty; and promotes healthspan, Cell Metabolism (2026), https://doi.org/10.1016/j.cmet.2026.05.015

STAR★METHODS

KEY RESOURCES TABLE

REAGENT or RESOURCE	SOURCE	IDENTIFIER
Antibodies		
PPARα	Santa Cruz Biotechnology	Cat#sc398394; RRID: AB_2885073
PAX7	R&D System	Cat#MAB1675; RRID: AB_2159833
AKT	Cell Signaling Technology	Cat#9272; RRID: AB_329827
p-AKT(Ser47)	Cell Signaling Technology	Cat#9271; RRID: AB_329825
p70S6K	Cell Signaling Technology	Cat#9202; RRID: AB_331676
p-p70S6K(Thr389)	Cell Signaling Technology	Cat#9205; RRID: AB_330944
p-STAT5(Tyr694)	Cell Signaling Technology	Cat#9351; RRID: AB_2315225
H3	Cell Signaling Technology	Cat#9715; RRID: AB_331563
Vinculin	Cell Signaling Technology	Cat#4650; RRID: AB_10559207
GAPDH	Cell Signaling Technology	Cat#2118; RRID: AB_561053
NcoR1	Proteintech	Cat#20018-1AP; RRID: AB_10665360
Secondary Anti Rabbit	Abcam	Cat#205718; RRID: AB_2819160
Secondary Anti Mouse	Cell Signaling Technology	Cat#7076; RRID: AB_330924
Chemicals, peptides, and recombinant proteins		
Protease and phosphatase inhibitor cocktails	Thermo Scientific	Cat#1861281
Clarity Western ECL Substrate	Biorad	Cat#1705060S
D-(+)-Glucose	Sigma Aldrich	Cat#8769-100ml
Humulin R U-100	Lilly	Cat#0002-8215-01
DMEM without methionine and cysteine	Thermo Fisher Scientific	Cat#21013024
Glutamine	Thermo Fisher Scientific	Cat#35050061
Methionine	Inotiv-Envigo	Cat#10850
FGF21	R&D Systems	Cat#2539-FG
GH	Millipore Sigma	Cat#869008
Rapamycin	ApexBio	Cat#A8167
STAT5-In-1	MedChem Express	Cat#HY-101853
Fenofibrate	Cayman Chemical	Cat#10005368
DMSO	Sigma Aldrich	Cat#472301
Critical commercial assays		
β-Hydroxybutyrate	Cayman Chemical	Cat#700190
Total cholesterol	Cayman Chemical	Cat#10007640
Insulin	Crystal Chem	Cat#62100
LDL	Crystal Chem	Cat#79980
HDL	Crystal Chem	Cat#79990
GH	Crystal Chem	Cat#80587
GLP-1	Crystal Chem	Cat#81508
Adiponectin	R&D System	Cat#MRP300
Leptin	R&D System	Cat#MOB00B
IGF-1	R&D System	Cat#MG100
FGF21	R&D System	Cat#MF2100
Glucagon	R&D System	Cat#DGCG0
Methionine	Abcam	Cat#ab234041

(*Continued on next page*)

Please cite this article in press as: Fanti et al., Methionine-supplemented longevity diet increases growth hormone, GLP-1, and FGF21; reduces frailty; and promotes healthspan, Cell Metabolism (2026), https://doi.org/10.1016/j.cmet.2026.05.015

Continued

REAGENT or RESOURCE	SOURCE	IDENTIFIER
NE-PER Nuclear and Cytoplasmic Extraction Reagents	Thermo Fisher Scientific	Cat#78835
Pierce BCA Protein Assay Kits	Thermo Fisher Scientific	Cat#23225
RNeasy Mini Kit (50)	Qiagen	Cat#74104
Deposited data		
Values used to create all graphs	Data S1-Source Data	N/A
RNAseq	This paper	GEO: GSE297351
Experimental models: Cell lines		
Primary mouse hepatocytes	Integrative Liver Cell Core at the Southern California Research Center for ALPD and Cirrhosis (Keck School of Medicine, USC)	N/A
Experimental models: Organisms/strains		
Mouse: CB6F1/J mice	Jackson Laboratory	Cat#100007
Mouse: C3D2F1/J mice	Jackson Laboratory	Cat#100004
Mouse: C57BL/6J mice	Jackson Laboratory	Cat#000664
Mouse: FGF21KO	Jackson Laboratory	Cat#033846
Mouse: GHRKO	Prof. J. Kopchick	N/A
Software and algorithms		
GraphPad Prism software, version 10.4.1	GraphPad software, San Diego, CA, USA	https://www.graphpad.com/
ImageJ (NIH) / Fiji software	Schindelin et al.[85]	https://imagej.net/software/fiji/
CalR v2 web-based tool	Mina et al.[36]	https://calrapp.org
R package, version 4.4.2	R Foundation for Statistical Computing	https://www.r-project.org/
Partek Flow Software	Illumina, Inc., San Diego, CA, USA	https://www.illumina.com/
Other		
Precision Xtra meter	Abbott Diabetes care	Cat#9881465
Precision Xtra Blood Glucose Test Strips	Abbott Diabetes care	Cat#7083
Precision Xtra Blood Ketone Test Strips	Abbott Diabetes care	Cat#7079
Mouse feeding jar	Dyets In.	Cat#910018

EXPERIMENTAL MODEL AND STUDY PARTICIPANT DETAILS

Mice

Genetically heterogeneous HET3 (UM-HET3) mice were used for longevity and healthspan. The mice were generated by crossing BALB/cJ x C57BL/6J F1 females (CB6F1/J) with C3H/HeJ x DBA/2J F1 males (C3D2F1/J), resulting in a four-way cross population. C57BL/6J (wild-type, WT), FGF21 knockout (FGF21KO), and growth hormone receptor knockout (GHRKO) mice were used for mechanistic studies. The C57BL/6J strain is one of four genetic backgrounds in HET3 mice and serves as the background for FGF21KO and GHRKO mice. FGF21KO and GHRKO mice originated from our colony. Littermates of the same sex were randomly assigned to experimental groups. Mice were group-housed (2–5 per cage) in ventilated cages with standard bedding and enrichment under specific pathogen–free conditions at 22°C temperature with a 12-hour light/12-hour dark cycle. Mice had unlimited access to water and food unless specified otherwise. All animal care and experimental procedures followed guidelines approved by the University of Southern California's Institutional Animal Care and Use Committee (IACUC).

Primary mouse hepatocytes

Primary mouse hepatocytes (HCs) were isolated from adult male C57BL/6 mice by the Integrative Liver Cell Core at the University of Southern California as described.[86]

METHOD DETAILS

Healthspan and longevity studies

At 20 months of age, the HET3 mice were randomized to either the healthspan study (30 females and 15-20 males per group) or the longevity study (40-44 females and 40-44 males per group). The enrollment period lasted 20 months. The healthspan cohort was assessed for metabolic and cognitive function and was euthanized for tissue collection after 5 months of intervention. Tissues

Please cite this article in press as: Fanti et al., Methionine-supplemented longevity diet increases growth hormone, GLP-1, and FGF21; reduces frailty; and promotes healthspan, Cell Metabolism (2026), https://doi.org/10.1016/j.cmet.2026.05.015

were collected from the mice in the FMD group after 4 days of refeeding. Body composition and frailty were assessed in both cohorts. Given the large number of tests to be conducted, and to ensure they were performed during the FMD refeeding periods, the evaluation of body composition, metabolism, behavior, and frailty was conducted at specific time points within a flexible few-week window. Mice were regularly monitored for any signs of stress or pain. For lifespan, the date of death was recorded for every mouse found dead or euthanized at the veterinarian's recommendation due to moribund criteria. Moribund criteria include one or a combination of the following: sustained hunched posture, respiratory difficulty, hypo/hyperthermia, ulcerated tumors, inability to access food or water, and inability to ambulate or make normal postural adjustments. Severe weight loss was also carefully evaluated along with other criteria. The date of euthanasia is taken as the best estimate of the date of natural death. Both euthanized mice and those found dead were represented as deaths in the survival curves. Each mouse found dead or euthanized was retained for possible inclusion in a necropsy study. Incisions were made in the cranium, thorax, and abdomen, and the entire body was immersed in 10% neutral buffered formalin and kept in a sealed container until autopsies were performed. All internal organs were dissected, sectioned, and examined macroscopically by the pathologist. Any abnormality was further examined under a dissecting microscope. Diagnosis of cancer was made primarily based on evidence of invasion of surrounding tissues or metastasis. Histopathological examinations were not performed. Because the study was conducted during the COVID-19 pandemic, vivarium access restrictions sometimes prevented the collection of carcasses. Therefore, the non-homogeneous number of autopsies among the groups may underestimate either the beneficial or detrimental effects of the diets on causes of death.

Mechanistic studies

Experiment on C57BL/6J mice: 15-month-old (n=4-5/group) and 12-month-old (n=4-5/group) female C57BL/6J wild-type (WT) mice were fed LD (methionine 0.14%) for 7 days (unless specified otherwise) before switching to SD (methionine 0.7%), LDMM (methionine 0.3%), or LDHM (methionine 0.7%) for an additional 7 days. Body composition was assessed at baseline, before switching, and at the end of the experiment, before tissue collection. Experiment on FGF21KO mice: 6-month-old female FGF21KO and 5-month-old WT mice (n=4/group) were fed LD for 7 days, then switched to LDMM for 5 more days. A separate group was fed LD for 12 days (n = 3). Body composition was assessed at baseline, before switching diets, and at the end of the experiment, before tissue collection. Experiment on GHRKO mice: 9-month-old female and male GHRKO mice and WT mice (n=6/group) were fed LD for 7 days before switching to LDMM for an additional 7 days. Tissues were collected at the end of the experiment.

Dietary interventions

The Standard (SD) or control diet is commercially available for mouse growth and maintenance. Energy Density: 3.1 Kcal/g; CHO 63%, Pro 24%, Fat 13%; ingredients: ground corn, soybean, ground wheat, ground oats, soybean oil, fishmeal, dried beet, dried whey (Pico5053, Research Lab) (Table S1). The Longevity Diet (LD) is a formulation that was developed to mimic the relatively low-protein diets that have been shown to extend the healthspan and lifespan of rodents,[70,87] diets emerging from epidemiological studies on healthspan and longevity,[68,88] as well as the eating habits and typical food choices of centenarians in Mediterranean areas[12] (customized by Envigo-Inotiv). Energy Density: 3.7 Kcal/g; CHO 58.8-58.1%, Pro 11.2-11.9%, Fat 30%; ingredients: vegetable mix (made with 15 vegetables), chickpeas, potato starch, fishmeal, fish oil, and olive oil. For experimental purposes, the Longevity Diet was provided at three methionine levels: low (no methionine supplementation, LD 0.14%), moderate (LDMM 0.3%), or high (LDHM 0.7%), matching the methionine levels in SD (Table S1). LD is also low in leucine (0.71%). Two additional versions of the diet were supplemented to match the same concentration of leucine in SD (1.5%): low methionine-high leucine (LD-high leu 1.5%) and moderate methionine-high leucine (LDMM-high leu 1.5%) (Table S2). The ketogenic diet (KD) is a formulation primarily composed of healthy food sources. Energy Density: 3.2 Kcal/g; CHO 8%, Pro 14%, Fat 78%; ingredients: apple, banana, fish, egg, white meat, coconut oil, almonds, walnuts, avocado, tomatoes, pepper (Table S1). The Western diet (WD) is formulated based on Western habits, characterized by high levels of refined sugars and saturated fats, with protein sourced primarily from animal products, and includes ingredients from popular fast-food restaurants. Energy Density: 2.62 Kcal/g; CHO 49%, Pro 13%, Fat 38%; ingredients: French fries, white bread, ketchup, chicken, bacon, egg, beef meat, butter, cheese, tomatoes, and onions (Table S1). The fasting-mimicking Diet (FMD) is a plant-based, calorie-restricted dietary regimen, typically ranging from 300 to 1100 kcal/day. Energy Density: 2.9 Kcal/g; CHO 47.7-55%, Pro 9-9.3%, Fat 36-43%; ingredients: broth powders, vegetable mix powder, extra virgin olive oil, and essential fatty acids. FMD was administered in 4-day cycles twice a month. At the end of the 4-day plan, or once mice show a 20% body weight loss, they are immediately refed ad libitum with the control diet (Pico5053, Research Lab) (Table S1). After the FMD cycle, the mice recover 95% of their original weight within 24 hours and 100% by 72 hours after refeeding. All diets were formulated and prepared in our laboratory, except for the Longevity Diet, which was customized by Envigo-Inotiv with ingredients we carefully selected.

Food intake, body weight, and body composition assessment

Body weight (BW) and food intake (FI) were measured twice a week unless otherwise noted. Because of the pellet's consistency, the LD often crumbled into small pieces and was provided in special jars (Dyets Inc., #910018) to ensure careful monitoring of food consumption. We excluded food intake records from cages in which the diet was entirely ground into powder and spilled in the cage. Body composition was measured using a noninvasive Nuclear Magnetic Resonance technique (LF90II Body Composition Analyzer,

Please cite this article in press as: Fanti et al., Methionine-supplemented longevity diet increases growth hormone, GLP-1, and FGF21; reduces frailty; and promotes healthspan, Cell Metabolism (2026), https://doi.org/10.1016/j.cmet.2026.05.015

LF90 time-domain nuclear magnetic resonance, TD-NMR; Bruker, USA). In the longevity and healthspan studies, it was measured at baseline and after 3 and 6 months of the intervention; in the short term studies, it was measured at baseline, before the diet change, and at the end of the experiment.

Indirect calorimetry analysis

After 3 months on experimental diets, 23-month-old female and male HET3 mice (n = 4-6/group) on SD, WD, KD, LDMM, and FMD were transferred to the PhenoMaster (TSE system) metabolic cages. The mice were housed individually in metabolic cages for nine consecutive days to record oxygen (O_2) consumption (mL/min), carbon dioxide (CO_2) production (mL/min), respiratory exchange ratio (RER, VCO_2/VO_2), energy expenditure (EE, kcal/h), and locomotor activity (total beam breaks, XT+YT), along with food consumption (kcal/day) and water intake (mL). Measurements were taken at 30-minute intervals throughout the entire period. The analysis presents data collected after at least 2 days of acclimatization in the cages, resulting in 7 light-dark cycles. Metabolic activity evaluated in 12-month-old female C57BL/6J mice (n = 3/group) was measured over 180 hours during the dietary transition from the LD to the LDMM diet.

Frailty Index Assessment

The frailty index (FI) score was calculated using the 31-item FI test[38] at 23 and 26 months of age. The severity of each item was rated on a scale of 0, 0.5, or 1. Each mouse was placed in a quiet evaluation room and allowed to acclimate for 30 minutes before scoring. The scorer was blinded to the mice's diet groups. Hearing loss was not assessed. Temperature was measured using an infrared thermometer. Scores were determined based on the number of standard deviations of the tested mouse relative to the mean weight of a 12-month-old mouse. Body weight was excluded from the frailty score because a) body mass changes are among the primary outcomes of the study, and b) it positively correlates with the frailty index (Figure S3N). The final FI score was calculated using a 29-item scale.

Glucose Tolerance Test (GTT) and Insulin Tolerance Test (ITT)

The GTT and ITT tests were conducted at 24 months of age during the refeeding after the FMD diet. Before testing, the mice were fasted for 4 to 5 hours and had free access to water. For the GTT, a 20% glucose solution was administered orally via gavage at a dose of 2 g/kg body weight. For the ITT, insulin was injected intraperitoneally at a dose of 0.5 U/kg body weight. Serial blood glucose measurements were taken at baseline (before gavage or injection) and at the indicated time points using a handheld glucometer and glucose strips. The meter has a reportable range of ~20–500 mg/dL. When glucose levels were at or above the limit ("low", <20mg/dL), the mice received a 20% glucose solution via gavage immediately.

Circulating markers

Mice were fasted for 4 to 6 hours and had free access to water before tissue collection at 25 months of age, following 5 months of dietary interventions. Tissue collections were performed on day 4 of refeeding after 10 cycles of FMD. All samples were collected between 10:00 a.m. and 2:00 p.m. Glucose and ketone body levels were determined using a handheld glucometer (Abbott, USA). Blood was processed for serum or plasma by centrifugation at 2000 × g for 20 minutes, then stored at -80 °C. Circulating markers were measured by ELISA, following the manufacturer's instructions. The HOMA-IR index was calculated as (fasting insulin)*(fasting glucose)/22.5. GH measurements were performed on samples collected after 4-5 hours of fasting during the light phase, when the mice are generally inactive and GH levels are more consistent and less affected by pulsatility.[89]

Novel Object Recognition Test

All behavioral and physical tests were conducted after 4 months on diets during the refeeding of mice following the FMD diet.

The novel object recognition (NOR) test[90] took place in a behavioral testing room, isolated from the researcher, with overhead lighting (180 lux) to avoid shadows. The open field arena, a plastic box, measured 61 cm x 36 cm x 30 cm, with two identical objects measuring 5 cm x 5 cm x 5 cm. The arena and objects were cleaned with 70% ethanol between trials to remove olfactory cues. The NOR test was conducted over two days, starting at 9:00 a.m. after a 1-hour acclimation period. On Day 1, the mice were allowed to explore the empty arena for 5 minutes. On Day 2, they explored the same arena with two identical objects for another 5 minutes (trial 1). After a 15-minute interval in their home cages, the mice returned for another 5 minutes, during which one object was replaced with a novel object of similar size but a different shape (trial 2). Exploration time was automatically recorded using EthoVision XT, which defined exploration as the mouse's head oriented towards the objects within 1.5 cm. The discrimination index (DI) was calculated as (TN - TF)/TT, where TN is the time spent on the novel object, TF is the time spent on the familiar object, and TT is the total time spent exploring both objects. Positive DI values indicate a preference for the novel object.

Barnes Maze

Barnes-Maze test[91] was performed in a behavioral testing room, separated from the researcher. The area was illuminated by overhead lighting (~1000 lux) above a white circular platform (91 cm in diameter) featuring 20 holes (5 cm in diameter) located 2.5 cm from the perimeter. Among these holes, only one was large enough for a mouse to enter (the escape box) and could be repositioned. Each mouse was assigned a specific escape box, which remained constant throughout the experiment. The platform was surrounded by three distal visual cues: 50-cm x 50-cm posters. During trials, background white noise of 90 dB was emitted from a loudspeaker. The

Please cite this article in press as: Fanti et al., Methionine-supplemented longevity diet increases growth hormone, GLP-1, and FGF21; reduces frailty; and promotes healthspan, Cell Metabolism (2026), https://doi.org/10.1016/j.cmet.2026.05.015

mice were assessed at 9 am, 1 hour after entering the experimental room. The test lasted 14 days, during which training occurred from days 1 to 7, followed by final testing on day 14. Training and testing sessions were separated by 15-minute intervals, with animals returned to their home cages. Each trial began at the center of the platform after 15 seconds in a chamber, ensuring no initial location cues. Mice explored the platform in search of the escape box; if unsuccessful within 2 minutes, the researcher gently guided the mouse into it, turned off the white noise, and allowed it to stay for 30 seconds. Testing was similar; if the mouse failed to find the escape box, it was returned to the home cage. On each experimental day, parameters recorded and averaged over the two tests included: success rate (100% or 0%, indicating the ability to find the escape box within two minutes), latency (time taken to locate the escape box), errors (nose pokes and head deflections at false holes), deviation (distance from the escape box at the first error), and strategies employed to locate the escape box (random, serial, or spatial).

Y-Maze

The Y-maze test was performed in a behavioral room, isolated from the researcher, and was illuminated with overhead lighting (~180 lux) above a Y-shaped maze with arms measuring 21 cm in length, 4 cm in width, and 4 cm in height. It began at 9 am after the mice had acclimated for 1 hour. The maze was cleaned with 70% ethanol between trials to eliminate olfactory cues. The test began by placing the mouse in a designated arm, facing the center, and allowing it 8 minutes of exploration. Total arm entries, defecation incidents, and arm choices for each mouse were recorded. Arm entry was defined as the mouse fully entering an arm with both fore and hind paws. Based on the order of arm entries, three scores were calculated: spontaneous alternation behavior percentage (SAB %), the percentage of consecutive entries into all three arms without repetitions (e.g., ABC, BCA); alternate arm return percentage (AAR %), the percentage of returns to the first visited arm (e.g., ABA, BAB); and same arm return percentage (SAR%), the percentage of returns to the same arm just exited (e.g., AAB, AAC).

Grip Strength

The grip strength test[90] was performed at 9 am in a room where the mice had been acclimated for one hour. Mice were held by the tail and allowed to grip the pull bar of the grip strength meter. While in a horizontal position, they were pulled backward until they released their grip, and the meter value was recorded. This process was repeated 3 times at 1-minute intervals, and the highest grip strength was used for analysis. Later that day, the mice were weighed and underwent NMR analysis to determine lean body mass. Strength was assessed and adjusted according to body weight and lean mass.

Rotarod

The rotarod test was conducted using the apparatus (Letica LE8200, Panlab, Barcelona, Spain), which consisted of a 3-cm-diameter rotating drum positioned 15 cm above the base. The assessment took place over two consecutive days at 9:00 a.m. in a designated room, where the mice were acclimated for 1 hour before testing. The apparatus was sanitized with 70% ethanol between trials and mice to eliminate olfactory distractions. On the first day, the training day, the mice underwent three training trials on the rotarod set at a constant speed of 4 rpm, remaining on the rod for at least 60 seconds and no more than 300 seconds. The following day, the testing day, the mice completed three trials on an accelerating rotarod (4-40 rpm) for up to 300 seconds. The time to fall during each trial was recorded. On the same day, after testing, the mice were weighed and underwent NMR analysis to determine lean body mass. The average fall time, based on the three trials, and the fall time adjusted for body weight and lean body mass were then calculated.

Protein analysis

Total protein lysates were extracted from liver and muscle tissues or primary hepatocytes with ice-cold radioimmunoprecipitation assay (RIPA) lysis buffer supplemented with protease and phosphatase inhibitor cocktails. The lysates were clarified by centrifugation at 15,000 rpm for 15 minutes, and protein concentrations were determined using the BCA method. Liver nuclear and cytoplasmic proteins were extracted using the NE-PER kit following the manufacturer's instructions. Western blots were performed as previously described.[92]

RNA extraction, sequencing, and data analysis

Total RNA was isolated from the livers of SD and LDLM→MM mice (n=5/group) after 5 months of diet for RNA sequencing using the RNeasy MINI Kit (Qiagen, Venlo, The Netherlands), following the manufacturer's protocol. Library preparation (poly A-enriched) and bulk RNA sequencing were performed by Novogene (Beijing, China). Messenger RNA was purified from total RNA using poly-T oligo-attached magnetic beads. After fragmentation, the first strand cDNA was synthesized using random hexamer primers, followed by the second strand cDNA synthesis using either dUTP for directional library or dTTP for non-directional library. For the non-directional library, it was ready after end repair, A-tailing, adapter ligation, size selection, amplification, and purification. The directional library was ready after end repair, A-tailing, adapter ligation, size selection, USER enzyme digestion, amplification, and purification. The library was checked using Qubit and real-time PCR for quantification, and a Bioanalyzer for size distribution detection. Libraries were pooled and sequenced on the Illumina NovaSeq 6000 PE150 platform following the manufacturer's guidelines. Raw data (raw reads) of fastq format were first processed through in-house perl scripts. In this step, clean data (clean reads) were obtained by removing adapters, poly-N, and low-quality reads from the raw data. At the same time, Q20, Q30, and GC content of the clean data were calculated. All the downstream analyses were based on clean, high-quality data. FASTQ files for each of the 10 samples were uploaded to Partek Flow (Illumina) for downstream gene expression analysis and data visualization. Pre-alignment quality assurance/quality

Please cite this article in press as: Fanti et al., Methionine-supplemented longevity diet increases growth hormone, GLP-1, and FGF21; reduces frailty; and promotes healthspan, Cell Metabolism (2026), https://doi.org/10.1016/j.cmet.2026.05.015

control (QA/QC) was performed, and sequences were aligned to the Mus musculus mm39 reference genome using STAR. Gene expression levels were determined using a "Quantify to annotation model (Partek E/M)" that mapped aligned reads to the GencodeM32_GFP584 (Ensembl) annotation embedded in Partek to obtain gene and transcript counts. Features were filtered to exclude those with a maximum count <= 10 to remove uninformative genes, and counts were normalized to counts per million (CPM) to account for differences in sequencing depth between samples. Differentially expressed genes (DEGs) between LDMM and SD were identified by statistical analysis using DESeq2. Genes with a p-value < 0.05 and FC > 2 or < -2 were considered differentially expressed and used for downstream pathway and IPA analyses. Principal component analysis (PCA), hierarchical clustering/heatmaps, KEGG pathway enrichment analysis, and Gene Set Enrichment Analysis (GSEA) were also performed in Partek. The Gene Ontology (GO) resource platform (http://geneontology.org) was used to identify overrepresented biological processes (BP), molecular functions (MF), and cellular components (CC) in the samples of interest. DEGs were uploaded to the GO platform, and GO sets were generated using the PANTHER (Protein Analysis Through Evolutionary Relationships) Classification System. Alternatively, the Reactome Pathway Database (https://reactome.org) was also used to determine enriched pathways. GO sets and pathways with enrichment score >2 and p-value <0.05 were considered significant and biologically relevant. DEGs were also uploaded onto the Ingenuity Pathway Analysis (IPA) software (Qiagen) for downstream pathway analysis.

In vitro experiment

The liver of C57BL/6J mice was perfused in situ via the portal vein with Ca^{2+}-free HBSS/EGTA buffer at 37°C to flush blood and disrupt cell junctions, followed by collagenase perfusion in Ca^{2+}-containing HBSS at 37°C until the liver capsule softened. The liver was excised, hepatocytes mechanically liberated, and the suspension filtered through a 70 μm mesh. Hepatocytes were pelleted by centrifugation at 50 × g for 1 min, washed twice, and viability assessed by trypan blue exclusion (>85%). Purified HCs were plated at a density of 2 × 10 ^4 cells per well in 96-well plates and 3 × 10 ^5 cells per well in 6-well plates in DMEM without methionine and cysteine, supplemented with 1% glutamine and 5% FBS to promote attachment, and incubated at 37°C and 5% CO2. Four hours after isolation, the primary hepatocytes were treated with the following drugs in DMEM without methionine, cysteine, and FBS: 1) Methionine diluted in water and tested in serial dilutions from 300 to 9.3 μg/L for dose-response, or at a concentration of 70 μg/L for a single test dose; 2) 250 ng/ml FGF21, diluted in water; 3) 500 ng/ml GH diluted in water; 4) 100 nM Rapamycin diluted in DMSO; 5) 100 μM STAT5-In-1 diluted in DMSO; and 6) 400 μM Fenofibrate, diluted in DMSO. After 18 hours of incubation at 37 °C and 5% CO2, the conditioned media were collected for ELISA detection of IGF-1 and FGF21 (Figure S7D).

Epidemiological data

Amino acid intake was estimated using the USDA FoodData Central database (https://fdc.nal.usda.gov/), based on average daily serving values reported by Malik et al.[68] For each food category reported in the paper, we selected a representative food item from the USDA database that most accurately reflected its typical composition. The amino acid content for each selected item was then multiplied by the corresponding average serving/day value. Data are presented as means for continuous variables and percentages for categorical variables. When comparing quintile 5 to quintile 1, p-values were compared using t-tests for continuous variables and χ^2-tests for categorical variables. Percent of energy from protein (kcal/day) was estimated by multiplying grams of protein consumed per day by the number of kcal in one gram of protein (4 kcal/g) and dividing by total caloric intake. Energy-adjusted intakes of amino acids were used in the analyses.

QUANTIFICATION AND STATISTICAL ANALYSIS

GraphPad Prism 10.4.1 (GraphPad Software) was used for all statistical analyses. Normality and homogeneity of variance were assessed using the Shapiro-Wilk and Levene's tests, respectively. Normally distributed data with equal variances were analyzed by one-way ANOVA with Tukey's post-hoc test; data with unequal variances by Welch's ANOVA with Dunnett's T3 post-hoc test; and non-normal data by Kruskal-Wallis test with Dunn's post-hoc test. When two independent factors were examined simultaneously, two-way ANOVA was applied, followed by Tukey's post-hoc test. Error bars represent SEM; data are also presented as box-and-whisker plots (median, minimum, maximum) or scatter plots (median). All tests were two-sided. Significance levels are indicated as *p < 0.05, **p < 0.01, ***p < 0.001, and ****p < 0.0001. Indirect calorimetry data were analyzed using GraphPad Prism and the CalR v2 web-based tool (https://calrapp.org).[35,36] Densitometry was performed using ImageJ (NIH)/Fiji software. For lifespan, Kaplan-Meier survival curves were generated to estimate the survival distributions for each group. Differences between survival curves were evaluated with the log-rank test and all pairwise diet comparisons. Cox proportional hazards regression was performed in R (version 4.4.2; R Foundation for Statistical Computing) using the "survival" and "ggplot2" packages. We fitted one model per sex with the standard diet as the reference category. Proportional hazards were assessed with Schoenfeld residuals for each group relative to the standard diet SD.